

Lawrence Berkeley National Laboratory

LBL Publications

Title

A Cavity-Stabilized Oscillator with Two Feedback Circuits

Permalink

<https://escholarship.org/uc/item/35n311vm>

Author

Franck, Jack Vernon, M.S. Thesis

Publication Date

1955-09-01

Copyright Information

This work is made available under the terms of a Creative Commons Attribution License, available at <https://creativecommons.org/licenses/by/4.0/>

UNIVERSITY OF
CALIFORNIA

*Radiation
Laboratory*

A CAVITY - STABILIZED OSCILLATOR
WITH TWO FEEDBACK CIRCUITS

BERKELEY, CALIFORNIA

DISCLAIMER

This document was prepared as an account of work sponsored by the United States Government. While this document is believed to contain correct information, neither the United States Government nor any agency thereof, nor the Regents of the University of California, nor any of their employees, makes any warranty, express or implied, or assumes any legal responsibility for the accuracy, completeness, or usefulness of any information, apparatus, product, or process disclosed, or represents that its use would not infringe privately owned rights. Reference herein to any specific commercial product, process, or service by its trade name, trademark, manufacturer, or otherwise, does not necessarily constitute or imply its endorsement, recommendation, or favoring by the United States Government or any agency thereof, or the Regents of the University of California. The views and opinions of authors expressed herein do not necessarily state or reflect those of the United States Government or any agency thereof or the Regents of the University of California.

UNIVERSITY OF CALIFORNIA

Radiation Laboratory
Berkeley, California

Contract No. W-7405-eng-48

A CAVITY-STABILIZED OSCILLATOR
WITH TWO FEEDBACK CIRCUITS

Jack Vernon Franck

(M. S. Thesis)

September 28, 1955

A CAVITY-STABILIZED OSCILLATOR
WITH TWO FEEDBACK CIRCUITS

Contents

Abstract	3
I. Introduction	4
II. Analysis of Pre-Exciter Oscillator	11
III. Calculation of Typical Operational Characteristics	19
A. Case I	19
B. Case II	30
C. Case III	36
D. Case IV	38
IV. Conclusions	48
V. Appendices	49
A. "Q" of grid circuit	49
B. Tube operation	55
C. Analysis of nonsinusoidal waves forms	60
D. Plate load impedance vs frequency	64
E. Impedance vector for a parallel resonant circuit	64
F. Experimental data	69
Definition of symbols	73
Graphical calculators	77
Bibliography	80

A STUDY OF
A CAVITY-STABILIZED OSCILLATOR
WITH TWO FEEDBACK CIRCUITS

Jack Vernon Franck

Radiation Laboratory
University of California
Berkeley, California

September 28, 1955

ABSTRACT

The pre-exciter oscillator used on the Berkeley 32-Mev proton linear accelerator is studied analytically and experimentally. The oscillator operates on 202.55 megacycles, using a single power tetrode, and is equivalent to a two-stage amplifier with two feedback circuits. Feedback circuit number one is a broadly tuned circuit around the first stage. Feedback circuit number two is a sharply tuned circuit around both stages. Feedback circuit No. 2 includes the cavity resonator. The object is a reduction in the number of high-frequency power tubes required in a conventional system. The frequency bandwidth over which the oscillator will "pull" to the resonator frequency is calculated and is found to be in good agreement with the measured value. Graphical calculators have been devised and used to reduce the computation to a minimum. The analysis of a self-oscillating system with two feedback circuits is believed to be new.

I. INTRODUCTION

A Cavity-Stabilized Oscillator

This paper is a study of a cavity-stabilized oscillator with two feedback circuits. The oscillator studied is used to supply the radio-frequency pre-excitation to the high-Q cavity of the Berkeley 32-Mev* proton linear accelerator.³

Because this particular oscillator is used to supply pre-excitation to the "Linac" cavity it has been defined as the "pre-exciter oscillator," and will be so designated throughout this paper.

Purpose of the Pre-Exciter Oscillator

The pre-exciter oscillator as used on the Linac fulfills several requirements. It drives the radiofrequency load cavity through the multipactor region,³ it selects the correct mode of oscillation, and it supplies the low level of radiofrequency voltage necessary to start the main power oscillators oscillating.

Requirements of the Pre-Exciter Oscillator

The pre-exciter oscillator should be frequency-stable and should deliver at least several percent of the normal output of the main power oscillators.

Design Specifications for the Pre-Exciter Oscillator

The pre-exciter oscillator under study was designed to conform to the following specifications:

Power output = 100 kilowatts,
Pulse length = 100 microseconds,
Repetition rate = 30 cycles per second,
Frequency = 202.55 megacycles per second,
Q (load) = 72,000
Plate voltage = 10,000 volts dc

In addition, during the "on" time of the main power oscillators the pre-exciter plate-circuit radiofrequency voltage is approximately

* million electron volts

five times the voltage existing during the pre-excitation period. This is shown by the following relations. (For definition of symbols see table, p. 74):

$$P_o = \frac{V_{ps}^2}{2 R_{ps}}, \quad V_{ps} = \sqrt{2 P_o R_{ps}}$$

$$\frac{V_{ps} \text{ (final level)}}{V_{ps} \text{ (pre-exc. level)}} = \sqrt{\frac{2400}{100}} = \sqrt{24} \cong 5.$$

The power output of the power oscillators is approximately 2400 kilowatts³ at a pulse length of 600 microseconds and a repetition rate of 15 pulses per second.

The pre-exciter plate circuit has to be able to withstand this high voltage if no "transmit-receive" switch is to be used. From Appendix B, page 56, this voltage is approximately

$$\begin{aligned} 5 V_{ps} \text{ (pre-exc. level)} &= 5 \times 4120 \\ &= 20,600 \text{ volts (crest).} \end{aligned}$$

Description of Pre-Exciter Oscillator

This pre-exciter oscillator is unique in that it has two feedback circuits. That is, it is a self-contained oscillator (cathode-grid-screen circuit) to which has been added a second feedback circuit. The line drawing, Fig. 1, shows the two feedback circuits.

In the particular pre-exciter under study, the complete function is filled by a single tetrode tube (4W20,000A) operating as a self-oscillator (cathode-grid-screen circuit) electron-coupled to the plate output circuit. A tetrode tube was selected for this particular installation since electrically and mechanically this results in the most economical and compact unit. In other applications separate tubes for each amplifier stage might be desirable. The resonant load is the cavity resonator of the Berkeley proton linear accelerator. The complete pre-exciter and its internal parts are shown photographically in Figs. 2 and 3. The U-shaped transmission line protruding from the pre-exciter oscillator

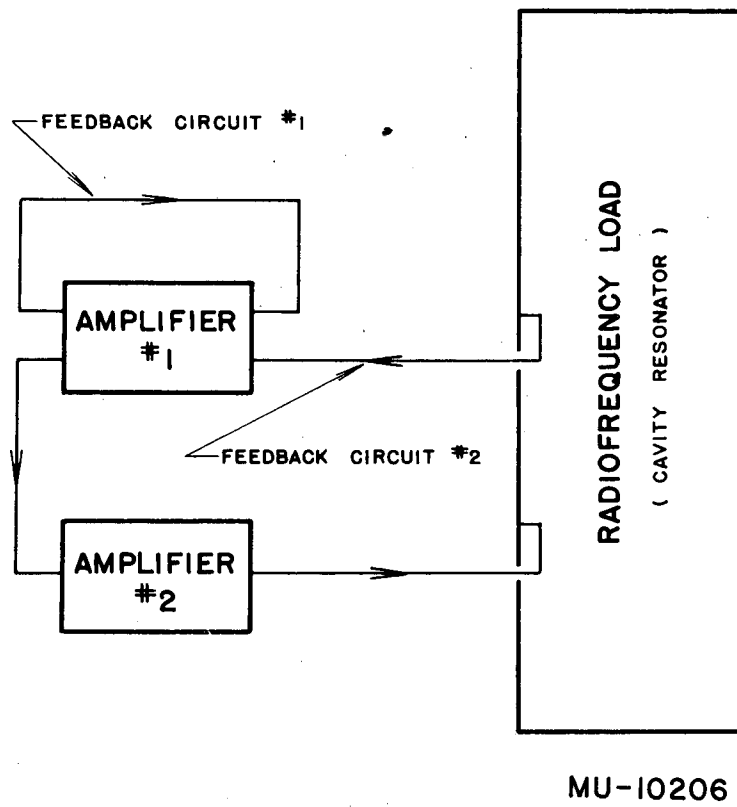
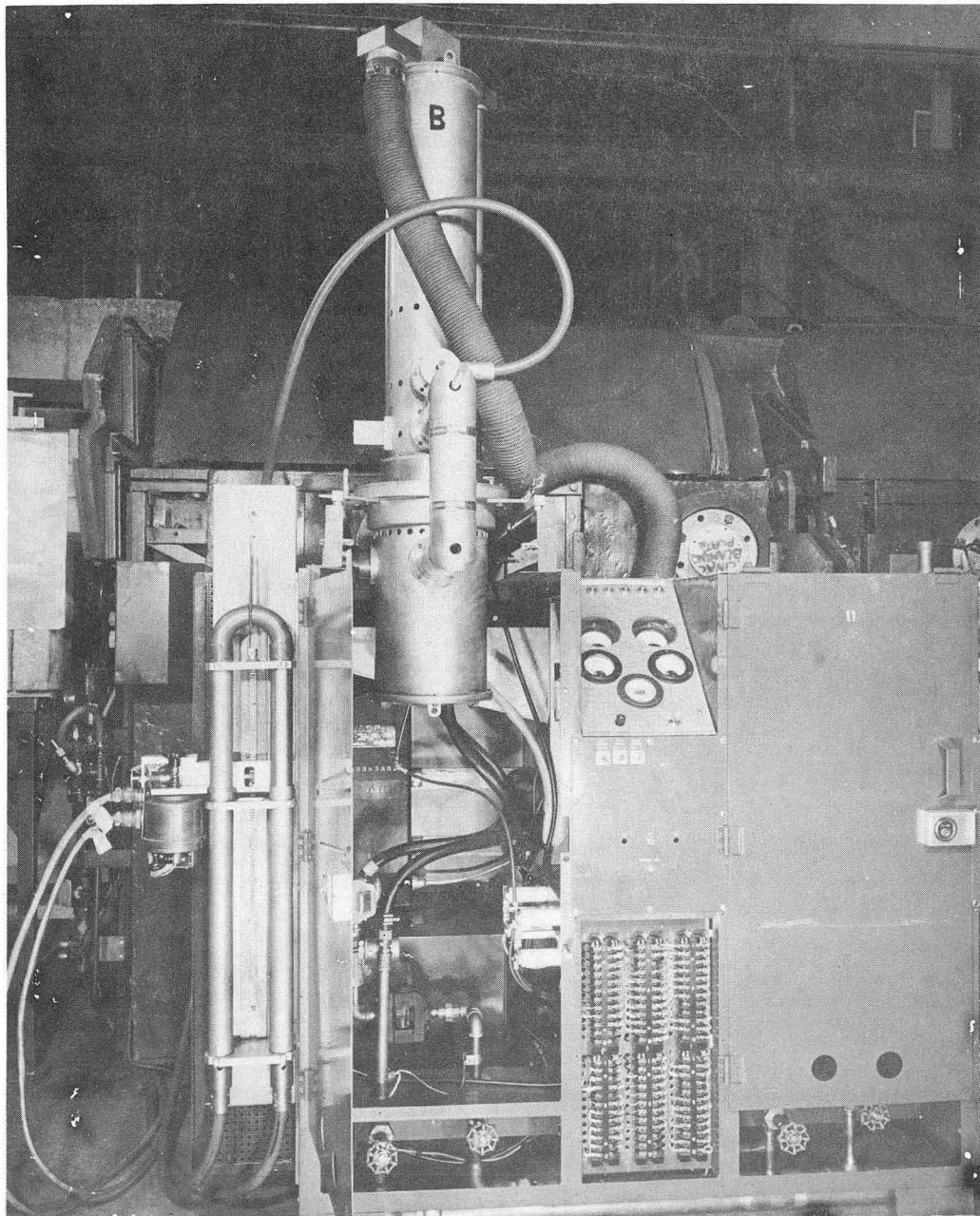
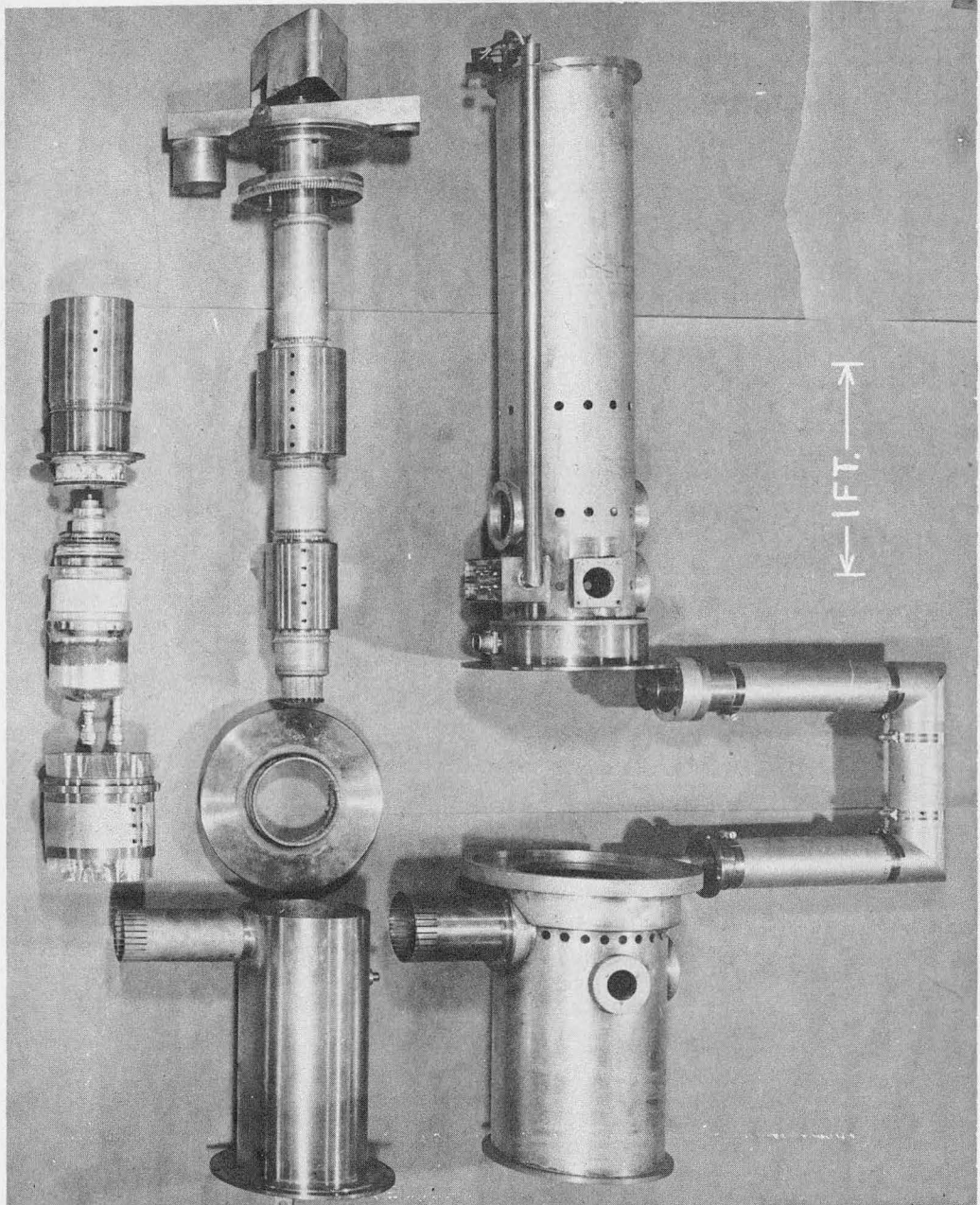


Fig. 1. Pre-exciter circuit.



ZN-1396

Fig. 2. Pre-exciter oscillator.



ZN-1395

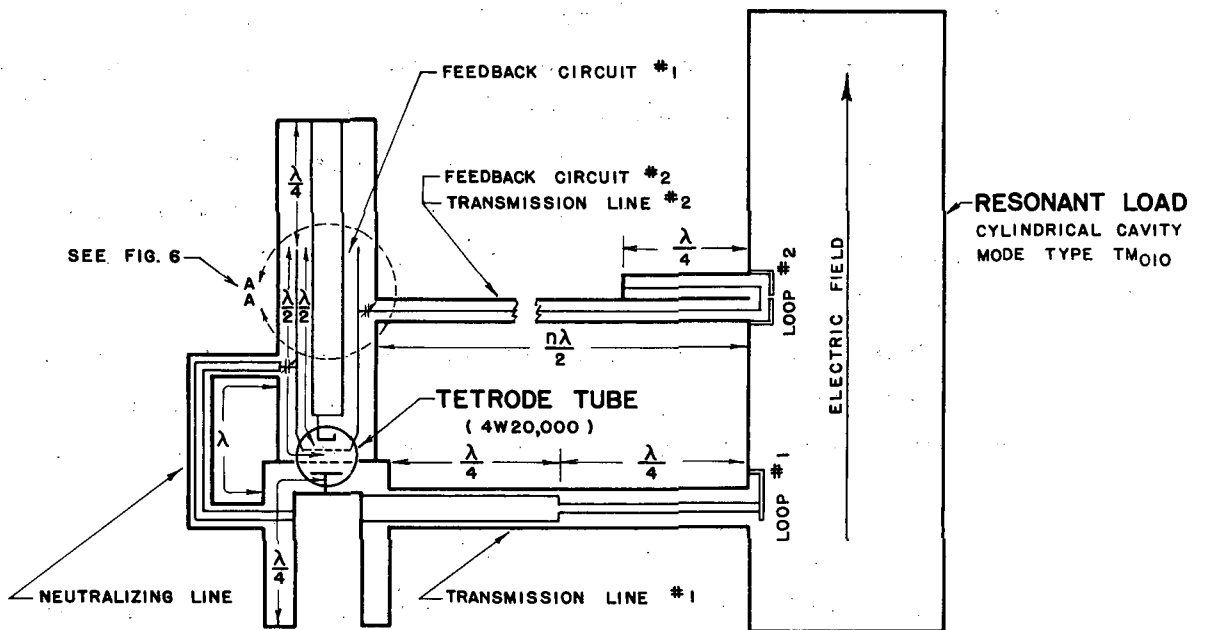
Fig. 3. Pre-exciter internal parts.

is used solely for neutralizing the plate to grid capacity.

Method of Operation

In actual operation, the pre-exciter oscillator is turned on about 100 microseconds prior to turning on the main power oscillators. During this time the pre-exciter builds the rf cavity voltage up to the 100-kilowatt level.

When the pre-exciter is first turned on there is no energy in the rf cavity. However, the cathode-grid-screen circuit starts oscillating vigorously in a relatively few cycles. This self-oscillating portion of the circuit is represented in the line drawing, Fig. 1, by amplifier No. 1 and feedback circuit No. 1. Since the tube is neutralized (see Fig. 4) the oscillating grid circuit is unaffected by voltage in the plate output circuit. Feedback circuit No. 2 is very loosely coupled to the grid circuit and therefore affects the level of oscillation very little. The self-oscillating cathode-grid-screen circuit delivers a fully modulated space current to the output plate circuit. This is independent of whether or not the oscillating frequency is the same as the natural resonant frequency of the plate load circuit. If the grid circuit is oscillating near the natural resonant frequency of the load, some voltage, however small, will be developed as a result of the flow of plate current. Feedback circuit No. 2 couples a portion of this load voltage back to the oscillating circuit. This feedback acts on the grid circuit as a frequency-correcting voltage in such a manner that the frequency of oscillation tends to be "pulled" toward the natural resonant frequency of the cavity-resonator load circuit. The amount of pulling and the manner in which this pulling occurs is the subject of study of this paper.



MU-10207

Fig. 4. Schematic diagram of pre-exciter oscillator.

II. ANALYSIS OF PRE-EXCITER OSCILLATOR

The following analysis uses equivalent lumped constants to represent the circuitry of the pre-exciter oscillator. The self-oscillating grid circuit and the feedback circuit are each represented by a simple generator with the appropriate internal impedance. Thevenin's theorem⁷ is the basis of this representation.

The equivalent circuit of the oscillator is defined by the geometry of the experimental equipment. The geometry is, in turn, defined by the conditions necessary for proper operation of the tube. A typical set of operating conditions for the tube is evaluated in Appendix B. The schematic diagram of the oscillator is shown in Fig. 4. A schematic diagram using lumped constants is shown in Fig. 5. The equivalent lumped-constant circuit is given in Fig. 6.

Some of the equivalent circuit voltages and impedances will be expressed in terms of the tube currents and plate-load impedance. The dependence of the plate-load impedance on frequency has been determined in Appendix D.

The network representing the feedback circuit is considered first.

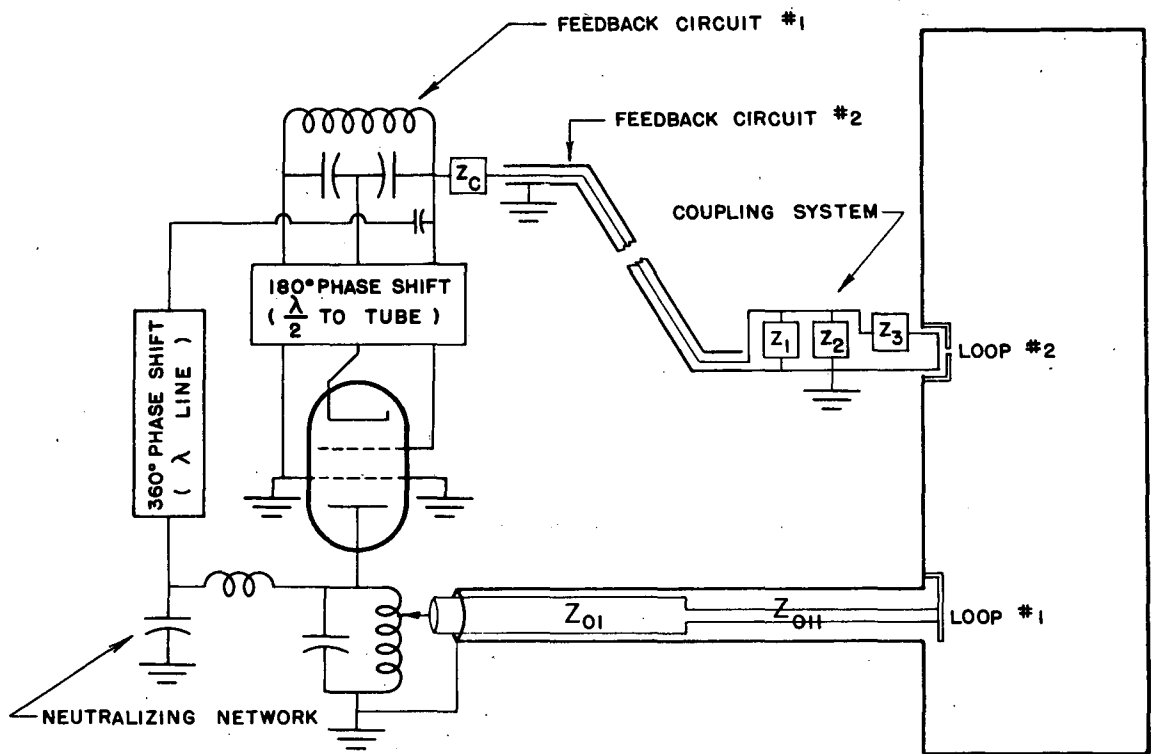
The voltage V_{fb} fed back to the grid circuit can be expressed in terms of the plate current and plate-load impedance of the tube:

$$V_{ps} = I_{ps} Z_{ps} \quad (1)$$

Transmission line No. 1 is constructed of two quarter-wave sections of different impedance and is connected to the plate line at a voltage $h V_{ps}$, where $h < 1.0$. The voltage on loop No. 1 is then

$$V_{\ell 1} = \frac{Z_{011}}{Z_{01}} h V_{ps} \quad (2)$$

Since the magnetic flux density is a constant along the side of a cylindrical resonator excited in the electric 010 mode, the voltages across all loops along the side are proportional to their areas:



MU-10208

Fig. 5. Schematic diagram of pre-exciter oscillator using lumped constants.

$$V_{\ell 1} / V_{\ell 2} = A_{\ell 1} / A_{\ell 2},$$

$$V_{\ell 1} = (A_{\ell 1} / A_{\ell 2}) V_{\ell 2}. \quad (3)$$

It is now convenient to define a coupling coefficient, c , which is determined by the adjustment of the network containing transmission line No. 2:

$$V_{fb} = c V_{\ell 2} \quad (4)$$

Writing Eq. (4) in terms of Eqs. (3), (2), and (1) gives

$$V_{fb} = hc \frac{A_{\ell 2}}{A_{\ell 1}} \frac{Z_{011}}{Z_{01}} \left[I_{ps} Z_{ps} \right] \quad (5)$$

The internal impedance Z_{fb} of feedback circuit No. 2 can now be evaluated. A power equality may be used to determine Z_{fb} in terms of Z_{ps} . At the natural resonant frequency of the load, the power generated by the tube is equal to the power delivered to the resonator via loop No. 1:

$$P_o = \frac{V_{ps}^2}{2R_{ps}} = \frac{V_{\ell 1}^2}{2Z_{\ell 1}(f_0)}. \quad (6)$$

From Eq. (6), by using the universal resonance curves,⁷ we obtain (see Appendix D.)

$$Z_{\ell 1} = \left[\frac{V_{\ell 1}}{V_{ps}} \right]^2 Z_{ps}. \quad (7)$$

Using Eq. (2), we have

$$Z_{\ell 1} = \left[\frac{Z_{011} h}{Z_{01}} \right]^2 Z_{ps}. \quad (8)$$

Since the voltage of loop No. 2 is the same as if the power were being put into the tank through loop No. 2, the relations between the voltages and the impedances can be again determined as in Eqs. (6) and (7):

$$V_{\ell 1}^2 / Z_{\ell 1} = V_{\ell 2}^2 / Z_{\ell 2},$$

$$Z_{\ell 2} = (V_{\ell 2} / V_{\ell 1})^2 Z_{\ell 1}. \quad (9)$$

Using Eqs. (3) and (8), we get

$$Z_{\ell 2} = (A_{\ell 2} / A_{\ell 1})^2 (Z_{011} h / Z_{01})^2 Z_{ps} \quad (10)$$

and from the coupling system schematic diagram (Fig. 7) it is evident that the feedback impedance has the form

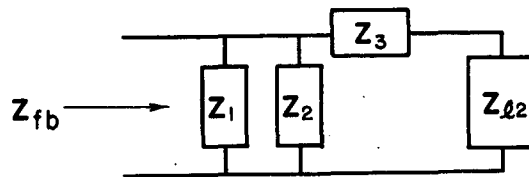
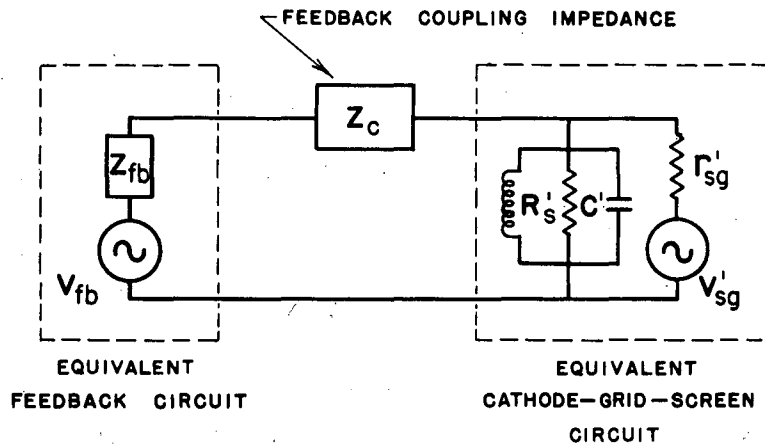
$$Z_{fb} = F(Z_1, Z_2, Z_3, Z_{\ell 2}, f). \quad (11)$$

The reactance Z_1 , is adjusted in magnitude by making transmission line No. 2 slightly longer or shorter than $\frac{n\lambda}{2}$. Similarly, Z_3 is a reactance the magnitude of which is determined by adjusting the quarter-wave line (associated with loop No. 2) to be slightly longer or shorter than $\frac{\lambda}{4}$. Z_2 is the equivalent shunt resistance of feedback transmission line No. 2.

This network has been interpreted from the experimental equipment. Once these impedances have been determined, Z_{fb} is found by solving the parallel-series network:

$$Z_{fb} = \frac{\left[Z_{\ell 2} + Z_3 \right] \left[\frac{Z_1 Z_2}{Z_1 + Z_2} \right]}{\left[Z_{\ell 2} + Z_3 \right] + \frac{Z_1 Z_2}{Z_1 + Z_2}} \quad (12)$$

The voltage V_{fb} (Eq. 5) and the impedance Z_{fb} (Eq. 12) are the open-circuit voltage and internal impedance respectively of a simple generator which by Thévenin's theorem can be used to represent



MU-10209

Figs. 6 and 7. Equivalent circuit of pre-exciter oscillator. Schematic diagram of feedback coupling system.

the feedback circuit. The voltage V'_{sg} and the resistance r'_{sg} represent the cathode-grid-screen circuit in the constant-voltage form of equivalent circuit for a vacuum tube. These are shown in Fig. 6.

The shunt resistance R'_s and the capacity C' of the equivalent grid circuit are referred to the point at which the feedback line is coupled. The voltage at this point is V_{02} (see Fig. 22).

The value of R'_s can be determined by solving for the dissipated power in the relations used to calculate the Q_t of the grid circuit. Using the relation for Q_t , which includes the grid drive power, gives for W_d (Appendix A)

$$W_d = \frac{\lambda r_s}{32 \pi} \left[8.46 \right] V_{02}^2 = \frac{V_{02}^2}{2 R'_s}$$

Expressing this in terms of a shunt resistance, we get

$$R'_s = \frac{32 \pi}{2 \lambda r_s} \left[\frac{1}{8.46} \right] = 563 \text{ ohms} \quad (13)$$

The value of C' may be determined from the Q_t (Appendix A) and the value determined for R'_s (Eq. (13)):

$$Q_t = \frac{\omega W_s}{W_d} = \frac{\omega \frac{C' V_{02}^2}{2}}{\frac{V_{02}^2}{2 R'_s}} = \omega C' R'_s$$

Solving for C' , we obtain

$$C' = \frac{Q_t}{\omega R'_s} = \frac{49.2}{2 \pi 202.55 \times 10^6 \times 563}$$

$$C' = 68.5 \times 10^{-12} \text{ farads.} \quad (14)$$

The value of r'_{sg} (see Fig. 6) is determined from the operating point for the tube (Appendix B) by transforming r_{sc} to the feedback point (V_{02}):

$$r_{sc} = \frac{e_{sm}}{I_{sg}} = \frac{2540}{70.1} = 36.6 \text{ ohms,}$$

$$r'_{sg} = r_{sc} \left[\frac{V_{05}}{V_{sc}} \right]^2 \left[\frac{V_{02}}{V_{05}} \right]^2 \quad (15)$$

The grid-to-screen voltage, $V_{sg} = V_{05}$, is the sum of the grid-cathode and screen-cathode voltages, since the screen voltage is 180° out of phase with the grid voltage:

$$V_{sg} = V_{05} = V_g + V_{sc}$$

From the tube operating point,

$$V_{sc} = 460 \text{ volts,}$$

$$V_g = E_g + e_{gm} = 1800 \text{ volts,} \quad (16)$$

therefore,

$$V_{sg} = V_{05} = 460 + 1800 = 2260 \text{ volts,} \quad (17)$$

$$\frac{V_{sg}}{V_{sc}} = \frac{V_{05}}{V_{sc}} = \frac{460 + 1800}{460} = \frac{2260}{460} = 4.92 \quad (18)$$

From Appendix A, $V_{05} = 0.667 V_{02}$, so

$$r'_{sg} = r_{sc} \left[\frac{V_{05}}{V_{sc}} \right]^2 \left[\frac{V_{02}}{V_{05}} \right]^2 = 36.6 \times 4.97^2 \times \frac{1}{0.667^2},$$

$$r'_{sg} = 1975 \text{ ohms.} \quad (19)$$

Since this circuit is self-oscillating, the fundamental frequency component of screen current is in phase with the grid-screen voltage. When it is normalized to voltage V_{02} this means that

$$V'_{sg} = I'_{sg} (R'_s + r'_{sg}). \quad (20)$$

The equivalent generator current I'_{sg} can be expressed in terms of the space current in the tube by normalizing to the tube voltage. These voltage ratios were calculated in evaluating r'_{sc} (Eqs. (16), (17), (18), (19)):

$$\begin{aligned} I'_{sg} &= I_{sg} \left[\frac{V_{sc}}{V_{05}} \right] \left[\frac{V_{05}}{V_{02}} \right] \\ &= I_{sg} \left[\frac{1}{4.92} \right] \left[.667 \right] = 0.135 I_{sg}. \end{aligned} \quad (21)$$

This gives for the equivalent generator voltage

$$\begin{aligned} V'_{sg} &= 0.135 I_{sg} (478 + 1975), \\ V'_{sg} &= 331 I_{sg}. \end{aligned} \quad (22)$$

The equivalent generator voltage can be expressed in terms of I_{ps} . Using the following ratio obtained from the calculation of tube operation, Appendix B, we get

$$\frac{I_{sg}}{I_{ps}} = \frac{70.1 \text{ amperes}}{55.0 \text{ amperes}} = 1.275; \quad (23)$$

the equivalent generator voltage is

$$\begin{aligned} V'_{sg} &= 331 \times 1.275 I_{ps}, \\ V'_{sg} &= 422 I_{ps}. \end{aligned} \quad (24)$$

Table I

Feedback voltage as a function of the frequency of oscillation

Δf_0 (cps)	Z_{ps} (ohms)	Z_{l2} (ohms)	Z_{l2} (ohms)	V_{fb} (volts)	V_{fb} (volts)
0	91.7/ 0°	117./ 0°	117. +j0.0	104./ $-30.0^\circ I_{ps}$	(+90.1-j52.0) I_{ps}
+470	87.1/ -18.5°	111./ -18.5°	105. -j35.4	98.7/ $-48.5^\circ I_{ps}$	(+65.4-j73.9) I_{ps}
-470	87.1/ $+18.5^\circ$	111./ $+18.5^\circ$	105. +j35.4	98.7/ $-11.5^\circ I_{ps}$	(+96.8-j19.7) I_{ps}
+705	82.5/ -26.5°	105./ -26.5°	94.4-j47.1	93.5/ $-56.5^\circ I_{ps}$	(+51.6-j77.9) I_{ps}
-705	82.5/ $+26.5^\circ$	105./ $+26.5^\circ$	94.4+j47.1	93.5/ $-3.5^\circ I_{ps}$	(+93.3-j5.7) I_{ps}
+1410	64.8/ -45.0°	82.9/ -45.0°	58.6-j58.6	73.5/ $-75.0^\circ I_{ps}$	(+19.0-j71.0) I_{ps}
-1410	64.8/ $+45.0^\circ$	82.9/ $+45.0^\circ$	58.6+j58.6	73.5/ $+15.0^\circ I_{ps}$	(+71.0+j19.0) I_{ps}
+2820	41.0/ -63.5°	52.5/ -63.5°	23.4-j46.9	46.5/ $-93.5^\circ I_{ps}$	(- 2.8-j46.4) I_{ps}
-2820	41.0/ $+63.5^\circ$	52.5/ $+63.5^\circ$	23.4+j46.9	46.5/ $+33.5^\circ I_{ps}$	(+38.8+j25.7) I_{ps}
+5640	22.2/ -76.0°	28.4/ -76.0°	69.0-j27.4	25.2/ $-106.0^\circ I_{ps}$	(- 6.9-j24.2) I_{ps}
-5640	22.2/ $+76.0^\circ$	28.4/ $+76.0^\circ$	69.0+j27.4	25.2/ $+46.0^\circ I_{ps}$	(+17.5+j18.1) I_{ps}
+11280	11.4/ -83.0°	14.6/ -83.0°	1.8-j14.5	12.9/ $-113.0^\circ I_{ps}$	(- 5.0-j11.9) I_{ps}
-11280	11.4/ $+83.0^\circ$	14.6/ $+83.0^\circ$	1.8+j14.5	12.9/ $+53.0^\circ I_{ps}$	(+ 7.8+j10.3) I_{ps}
+22560	5.7/ -86.5°	7.3/ -86.5°	0.4-j 7.3	6.5/ $-116.5^\circ I_{ps}$	(- 2.9-j 5.8) I_{ps}
-22560	5.7/ $+86.5^\circ$	7.3/ $+86.5^\circ$	0.4+j 7.3	6.5/ $+56.5^\circ I_{ps}$	(+ 3.6+j 5.4) I_{ps}
+45120	2.8/ -88.2°	3.6/ -88.2°	0.1-j 3.6	3.2/ $-118.2^\circ I_{ps}$	(- 1.5-j 2.8) I_{ps}
-45120	2.8/ $+88.2^\circ$	3.6/ $+88.2^\circ$	0.1+j 3.6	3.2/ $+58.2^\circ I_{ps}$	(+ 1.7+j 2.7) I_{ps}

All parts of the equivalent circuit (Fig. 6) have now been evaluated for Case I. The values are shown on the equivalent circuit diagram, Fig. 8. The frequency-dependent values are tabulated in Table I.

The superposition theorem⁷ can be used here to solve for the network currents i_1 , i_2 , and i_3 , from which the effect of the feedback network can be determined. This would have to be subjected to the restriction that $i_1 = I'_{sg}$ must be in phase with V'_{sg} , since this part of the circuit is a self-oscillator. It is to be noted, however, that the impedance of the equivalent cathode-grid-screen circuit is at most a few percent of the combined feedback and coupling impedances ($Z_{fb} + Z_c$). In this case I'_{sg} , to a good approximation, flows entirely through R'_s .

The feedback current i_3 , which by design is very small compared to I'_{ps} , will in general have an inphase and a quadrature component with respect to I'_{ps} . The quadrature component, as stated before, must flow only through the reactances of the equivalent cathode-grid-screen, resonant circuit. The inphase component of i_3 must divide between R'_s and r'_{sg} as a consequence of the use of the superposition theorem, subject to the approximation that $i_1 = I'_{sg}$ flows only through R'_s .

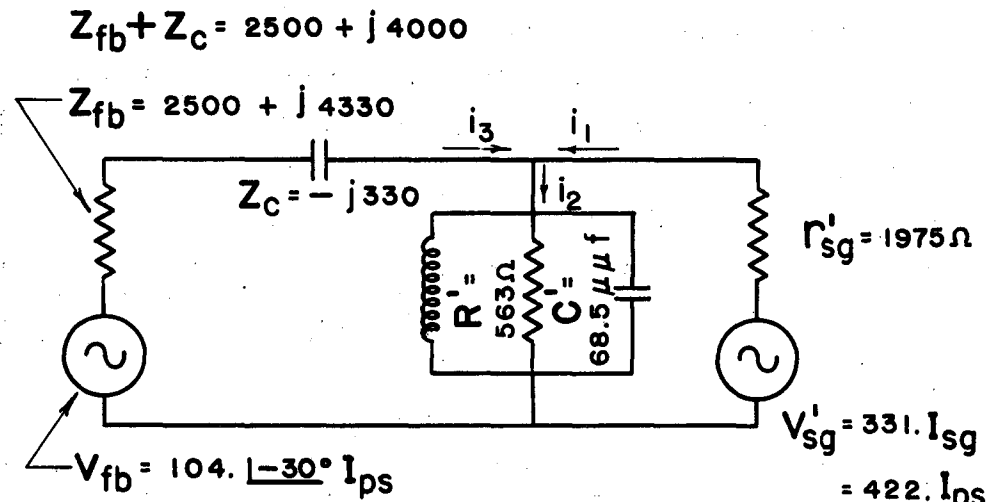
The current i_3 can be evaluated as a function of frequency as follows:

$$i_3 = \frac{-V_{fb} + V'_{rs}}{Z_{fb} + Z_c} = \frac{-V_{fb} + \left[\frac{R'_s}{R'_s + r'_{sg}} \right] V'_{sg}}{Z_{fb} + Z_c} \quad (25)$$

All values needed are constant or have previously been evaluated. V_{fb} has been calculated as a function of frequency and is tabulated in Table I for Case I. We have, therefore,

$$\begin{aligned} i_3 &= \frac{-V_{fb} + 93.6 I'_{ps}}{2500 + j4000} \\ &= \left[-V_{fb} + 93.6 I'_{ps} \right] \left[1.12 - j1.80 \right] 10^{-4} \quad (26) \end{aligned}$$

The current i_3 is tabulated as a function of frequency in Table II. The equivalent shunt capacity C'' , representing the quadrature component of the current i_3 , is also listed. This is obtained from the following



MU-10210

Fig. 8. Case I: equivalent circuit.

Table II

Case I. Frequency shift as a function of the frequency of oscillation

Δf_0 (cps)	I_3 (amp)	C_{II} (μuf)	C_{III} (μuf)	Δf (KC)
0	$(+97.4 + j52.2) 10^{-4} I_{ps}$	+0.044	0	0
+ 470	$(+164. + j32.3) 10^{-4} I_{ps}$	+0.028	-0.016	+23.6
- 470	$(+39.0 + j28.0) 10^{-4} I_{ps}$	+0.023	-0.020	+30.0
+ 705	$(+187. + j12.0) 10^{-4} I_{ps}$	+0.010	-0.033	+49.3
- 705	$(+10.6 + j 5.9) 10^{-4} I_{ps}$	+0.004	-0.039	+58.0
+1410	$(+212. - j54.4) 10^{-4} I_{ps}$	-0.046	-0.090	+133.
-1410	$(- 8.9 - j61.9) 10^{-4} I_{ps}$	-0.052	-0.096	+142.
+2820	$(+191. - j122.) 10^{-4} I_{ps}$	-0.102	-0.145	+215.
-2820	$(+ 3.8 - j127.) 10^{-4} I_{ps}$	-0.109	-0.152	+225.
+5640	$(+157. - j154.) 10^{-4} I_{ps}$	-0.128	-0.171	+254.
-5640	$(+53.1 - j157.) 10^{-4} I_{ps}$	-0.132	-0.176	+260.
+11280	$(+132. - j164.) 10^{-4} I_{ps}$	-0.137	-0.181	+268.
-11280	$(+77.8 - j165.) 10^{-4} I_{ps}$	-0.139	-0.183	+270.
+22560	$(+119. - j167.) 10^{-4} I_{ps}$	-0.141	-0.184	+273.
-22560	$(+91.5 - j168.) 10^{-4} I_{ps}$	-0.141	-0.184	+273.
+45120	$(+112. - j168.) 10^{-4} I_{ps}$	-0.141	-0.184	+273.
-45120	$(+98.6 - j168.) 10^{-4} I_{ps}$	-0.141	-0.184	+273.

relation (the inphase component of i_3 is completely negligible in comparison with the inphase current I'_{sg}):

$$C'' = \frac{i_3 \text{ (quadrature part)}}{w \left[\frac{R'_s}{R'_s + r'_{sg}} \right] 422 I_{ps}}$$

$$= \frac{i_3 \text{ (quadrature part)}}{w 93.6 I_{ps}} \quad (27)$$

The capacity C''' is the effective value of the capacity resulting from the feedback network after correcting the value of this capacity so that the oscillating circuit receives zero frequency correction when it is at the natural resonant frequency (f_0) of the load.

The frequency shift that occurs because the capacity C''' is in parallel with the grid circuit is evaluated as follows.

Let

$$f = \frac{1}{2\pi\sqrt{LC}} ;$$

$$f + \Delta f = \frac{1}{2\pi\sqrt{L(C + \Delta C)}} = \frac{1}{2\pi\sqrt{LC}\sqrt{1 + \frac{\Delta C}{C}}}$$

Since $\Delta f \ll f$, the following approximation can be made,

$$\frac{1}{\sqrt{1 + \frac{\Delta C}{C}}} \cong \frac{1}{1 + \frac{\Delta C}{2C}} \cong 1 - \frac{\Delta C}{2C} ,$$

and therefore

$$f + \Delta f = f \left[1 - \frac{\Delta C}{2C} \right] ,$$

or, for $f = f_0$, $\Delta C = C'''$, and $C = C'$ (see Fig. 8),

$$\Delta f = \left[-\frac{C'''}{2C'} f_0 \right] \quad (28)$$

The values of Δf are tabulated in Table II. The results of Case I are displayed in Fig. 9 along with the experimental values from Appendix F (Figs. 28 and 29). Figures 10 and 11 are merely the graphical solution of the relation $+f = \Delta f_0 - \Delta f$. Figure 9 is a plot of Δf_0 vs. f .

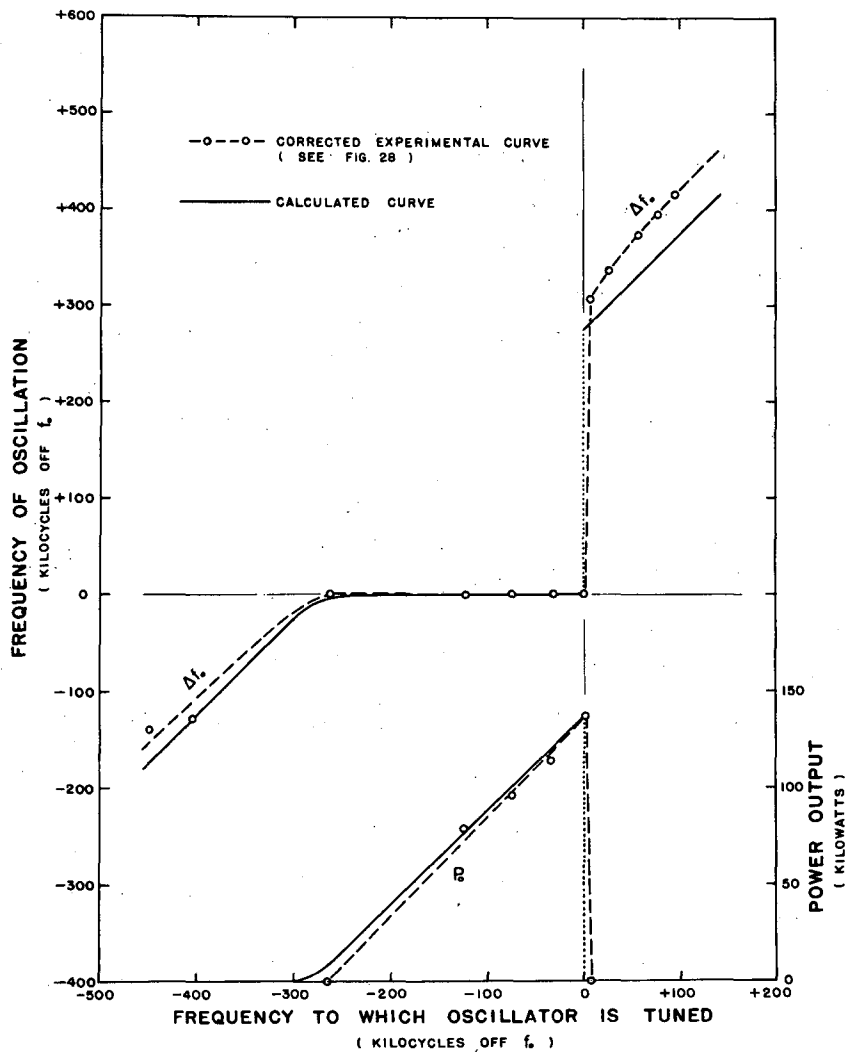
The power output of the oscillator as a function of frequency can be obtained by use of the relation

$$P_o(f) = \frac{I_{ps}^2 R_{ps}(f)}{2} \tag{29}$$

In this equation, I_{ps} is a constant (see p. 9) and $R_{ps}(f)$ has been evaluated in Appendix D. The power output as a function of frequency is tabulated in Table III and is plotted in Fig. 9 along with the experimental results of Appendix F.

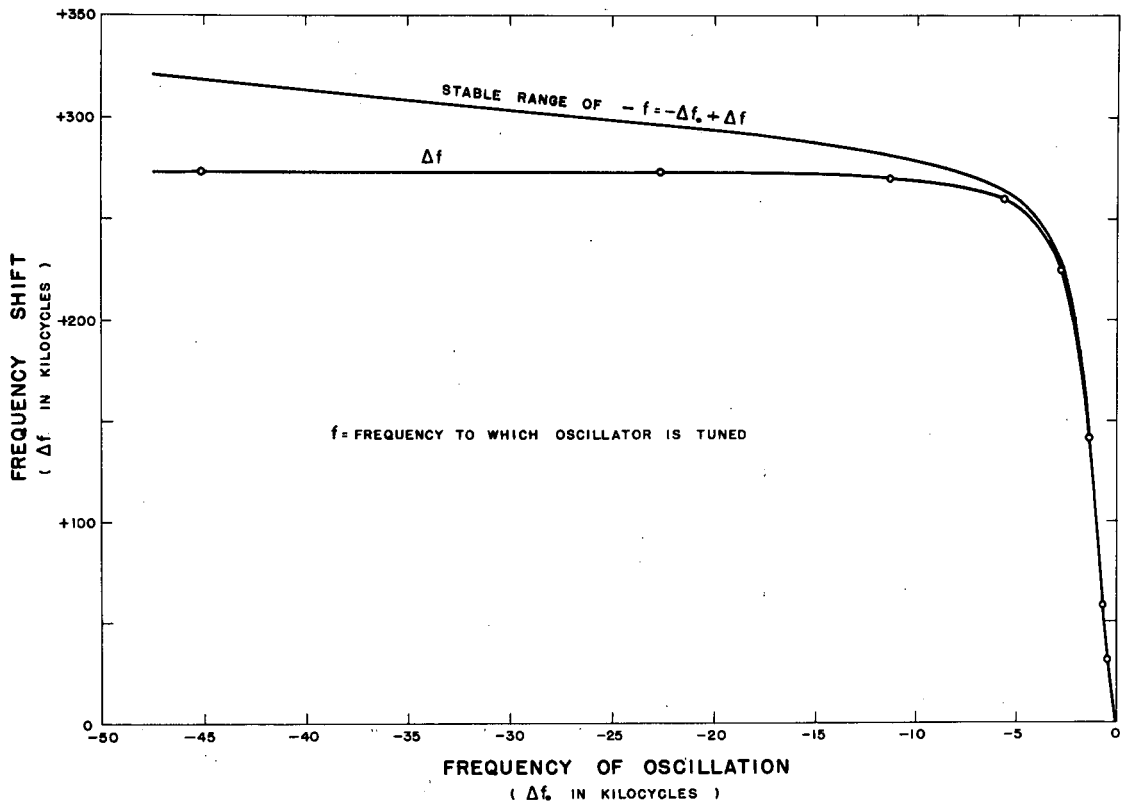
Table III

Power output as a function of frequency of oscillation	
Δf_0 (cps)	P_o (kw)
0	138.
± 470	125.
± 705	113.
±1410	69.
±2820	28.
±5640	8.
±11280	2.
±22560	0.5
±45120	0.1



MU-10211

Fig. 9. Case I: Frequency of oscillation and power output as functions of the frequency to which the oscillator is tuned.



MU-10212

Fig. 10. Case I: Relation between frequency of oscillation and frequency shift. (lower frequencies)

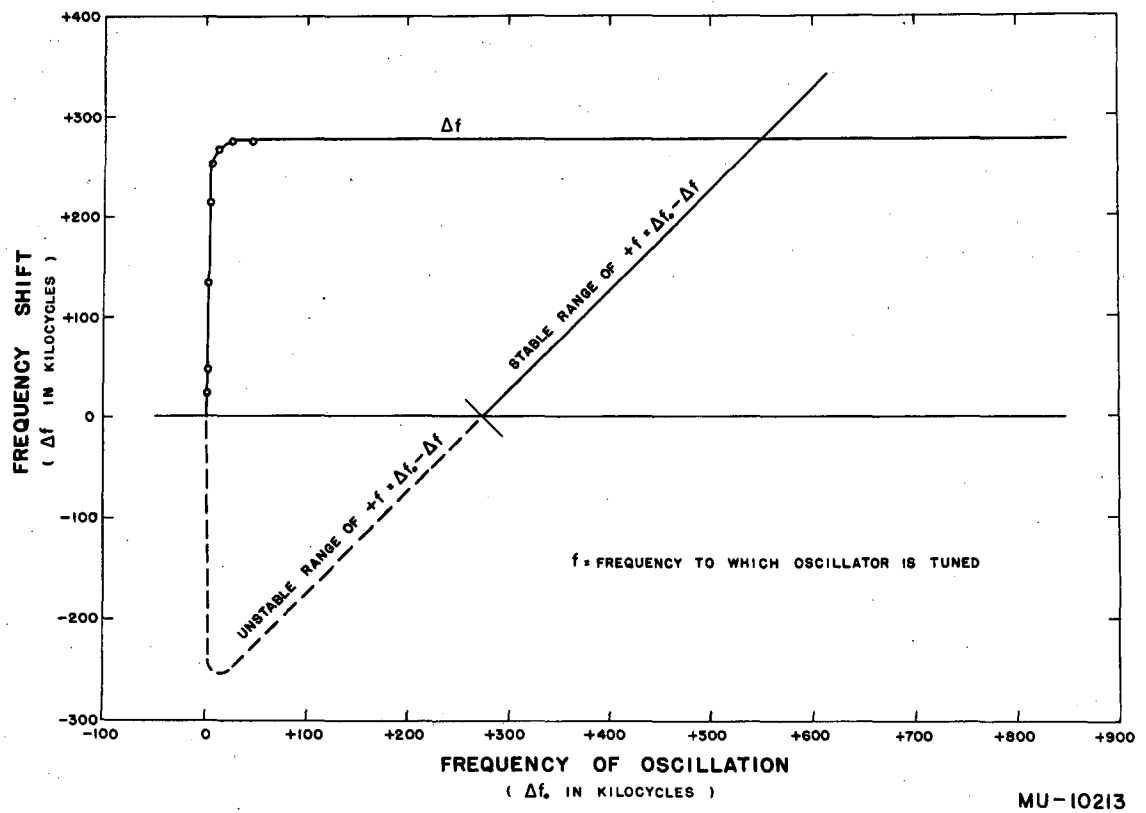


Fig. 11. Case I: Relation between frequency of oscillation and frequency shift (higher frequencies).

B. Case II

The conditions in Case II are identically the same as for Case I, except that much of the tedious vector computation is bypassed by using several graphical calculators. Illustrations of these calculators are found on pages 78 , 79 , and 80 . Their use was suggested and made possible by the fact that the internal impedance of the equivalent generator representing the feedback circuit is very large compared to the shunt impedance of the cathode-grid-screen circuit. The circular calculator is an expression of the fact that the locus of the impedance vector for a parallel resonant circuit is a circle. This is demonstrated in Appendix E.

To solve Case I with the graphical calculator, the grid circuit voltage V'_{rs} is drawn to unit length as indicated on graphical calculator No. 1. Calculator No. 1 is then rotated so that the feedback voltage has the desired phase angle with respect to the grid voltage V'_{rs} at the natural resonant frequency of the load circuit (f_0). Calculator No. 2, on which has been drawn the impedance line representing the total impedance in the feedback circuit ($Z_{fb} + Z_c$) in arbitrary units, is placed so that the origin is coincident with the head of the vector representing the feedback voltage V_{fb} . The magnitude of V_{fb} is relative to the unit length chosen for V'_{rs} . The impedance line is made to pass over the head of the vector representing the grid circuit voltage V'_{rs} . The relative magnitude of the feedback current (i_3), and its phase, can be read from calculator No. 2 by use of a protractor or calculator No. 3. Calculator No. 3 can be used to read the quadrature component of the feedback current directly from calculator No. 2 without bothering with the relative magnitude.

The feedback current for other frequencies is obtained in the same manner as above. The magnitude and phase of the feedback voltage as a function of frequency are read directly on calculator No. 1. The frequency is given in terms of the Q of the load. The Δf can be readily determined by referring to Appendix D.

The relative magnitude of the feedback voltage can be determined by referring to Table I, and Eq. (25). Then we have

$$\left| \frac{V_{fb}}{V'_{rs}} \right| = \frac{104.}{93.6} = 1.11 \quad (30)$$

A single numerical computation is required to find the normalizing constant for the current. This is done by evaluating Eqs. (25) and (26) for the natural resonant frequency of the load impedance (cavity resonator),

$$\begin{aligned} i_3 &= \frac{V'_{rs} - V_{fb}}{Z_{fb} + Z_c} = \frac{93.6 I_{ps} - V_{fb}}{2500 + j 4000} \\ &= \left[93.6 I_{ps} - 104 \angle -30^\circ I_{ps} \right] \left[1.12 - j 1.80 \right] 10^{-4} \\ &= \left[97.4 + j 52.2 \right] 10^{-4} I_{ps} \end{aligned} \quad (31)$$

The normalizing constant is

$$N = \frac{52.2 \times 10^{-4}}{.21} = 248. \times 10^{-4} \quad (32)$$

The equivalent shunt capacity C'' is by Eq. (27),

$$\begin{aligned} C'' &= \frac{i_3 \text{ (quadrature part)}}{\omega 93.6 I_{ps}} \\ &= \frac{i_3 \text{ (quadrature part)}}{I_{ps}} \times 0.839 \times 10^{-11} \end{aligned} \quad (33)$$

The value of C''' is found as in Case I, page 26, and the Δf is again obtained by use of Eq. (28).

The results as obtained by use of the graphical calculators are tabulated in Table IV, and are plotted in Fig. 12, as obtained from Figs. 13 and 14. For comparison, the analytical results of Case I are also plotted in Fig. 12.

Table IV

Case II. Frequency shift as a function of the frequency of oscillation

Δf_0 (cps)	$i_3 \times 1/N$ (amp)	$i_3 \times 1/N$ (quad. part) (amp)	i_3 (quad. part) (amp)	C'' ($\mu\mu\text{f}$)	C''' ($\mu\mu\text{f}$)	Δf (kc)
0	$0.47 / +27.0^\circ I_{ps}$	$0.21 / +90^\circ I_{ps}$	$+52.2 \times 10^{-4} / +90^\circ I_{ps}$	+0.044	0	0
+470	$0.71 / +11.0^\circ I_{ps}$	$0.14 / +90^\circ I_{ps}$	$+34.8 \times 10^{-4} / +90^\circ I_{ps}$	+0.029	-0.015	+21.8
-470	$0.18 / +39.5^\circ I_{ps}$	$0.12 / +90^\circ I_{ps}$	$+29.8 \times 10^{-4} / +90^\circ I_{ps}$	+0.025	-0.019	+27.5
+705	$0.80 / +3.5^\circ I_{ps}$	$0.05 / +90^\circ I_{ps}$	$+12.4 \times 10^{-4} / +90^\circ I_{ps}$	+0.010	-0.033	+49.3
-705	$0.05 / +12.7^\circ I_{ps}$	$0.01 / +90^\circ I_{ps}$	$+2.5 \times 10^{-4} / +90^\circ I_{ps}$	+0.002	-0.042	+62.3
+1410	$0.93 / -14.5^\circ I_{ps}$	$0.23 / -90^\circ I_{ps}$	$-57.1 \times 10^{-4} / +90^\circ I_{ps}$	-0.048	-0.091	+135.
-1410	$0.27 / -98.0^\circ I_{ps}$	$0.26 / -90^\circ I_{ps}$	$-64.5 \times 10^{-4} / +90^\circ I_{ps}$	-0.050	-0.099	+145.
+2820	$0.97 / -32.5^\circ I_{ps}$	$0.51 / -90^\circ I_{ps}$	$-127. \times 10^{-4} / +90^\circ I_{ps}$	-0.106	-0.149	+220.
-2820	$0.55 / -82.5^\circ I_{ps}$	$0.54 / -90^\circ I_{ps}$	$-137. \times 10^{-4} / +90^\circ I_{ps}$	-0.113	-0.157	+232.
+5640	$0.93 / -44.5^\circ I_{ps}$	$0.66 / -90^\circ I_{ps}$	$-164. \times 10^{-4} / +90^\circ I_{ps}$	-0.138	-0.181	+268.
-5640	$0.71 / -71.0^\circ I_{ps}$	$0.68 / -90^\circ I_{ps}$	$-169. \times 10^{-4} / +90^\circ I_{ps}$	-0.142	-0.186	+276.
+11280	$0.89 / -51.0^\circ I_{ps}$	$0.69 / -90^\circ I_{ps}$	$-171. \times 10^{-4} / +90^\circ I_{ps}$	-0.144	-0.187	+276.
-11280	$0.78 / -64.0^\circ I_{ps}$	$0.70 / -90^\circ I_{ps}$	$-174. \times 10^{-4} / +90^\circ I_{ps}$	-0.146	-0.191	+283.
+22560	$0.87 / -54.5^\circ I_{ps}$	$0.70 / -90^\circ I_{ps}$	$-174. \times 10^{-4} / +90^\circ I_{ps}$	-0.146	-0.191	+283.
-22560	$0.82 / -61.0^\circ I_{ps}$	$0.72 / -90^\circ I_{ps}$	$-179. \times 10^{-4} / +90^\circ I_{ps}$	-0.149	-0.193	+283.
+45120	$0.86 / -56.5^\circ I_{ps}$	$0.71 / -90^\circ I_{ps}$	$-176. \times 10^{-4} / +90^\circ I_{ps}$	-0.148	-0.191	+283.
-45120	$0.83 / -59.5^\circ I_{ps}$	$0.72 / -90^\circ I_{ps}$	$-179. \times 10^{-4} / +90^\circ I_{ps}$	-0.149	-0.193	+283.

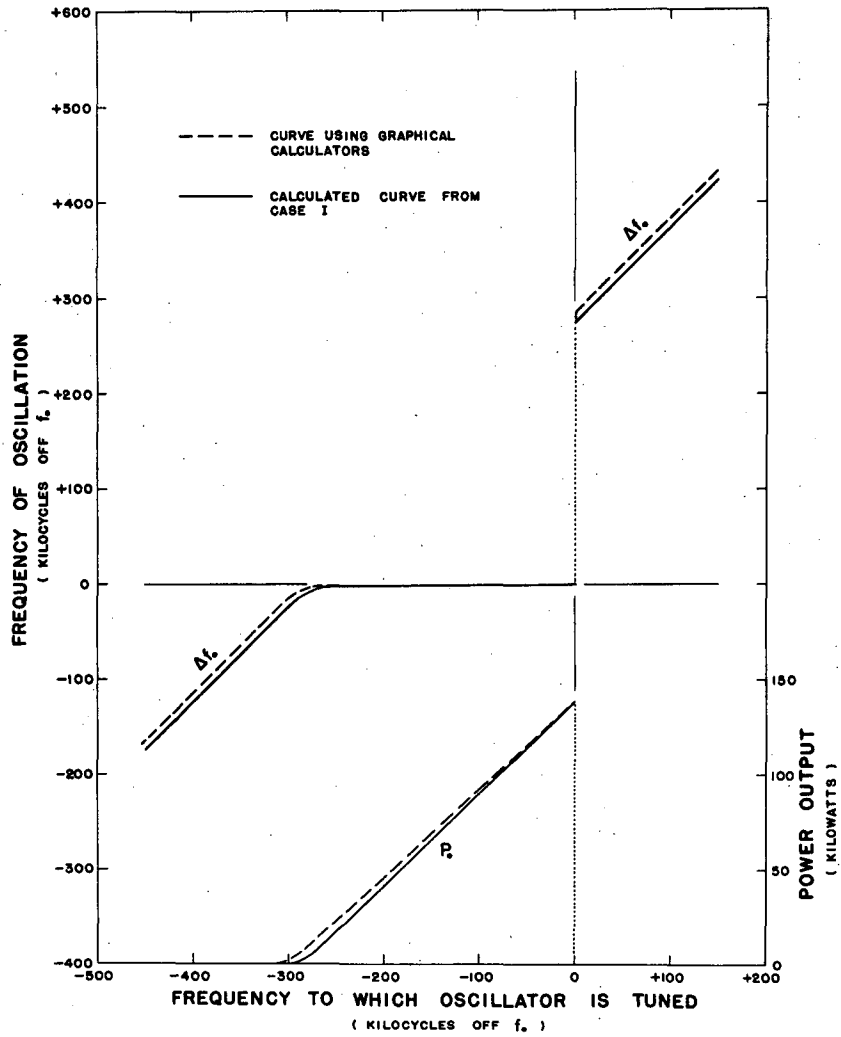
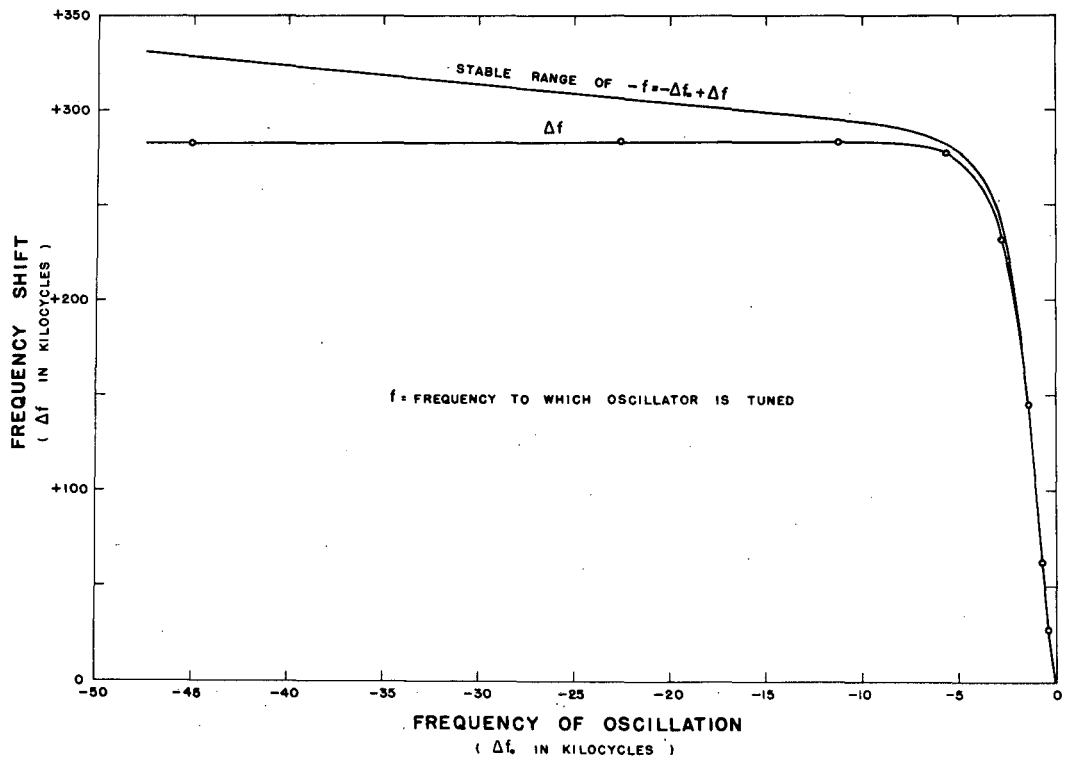
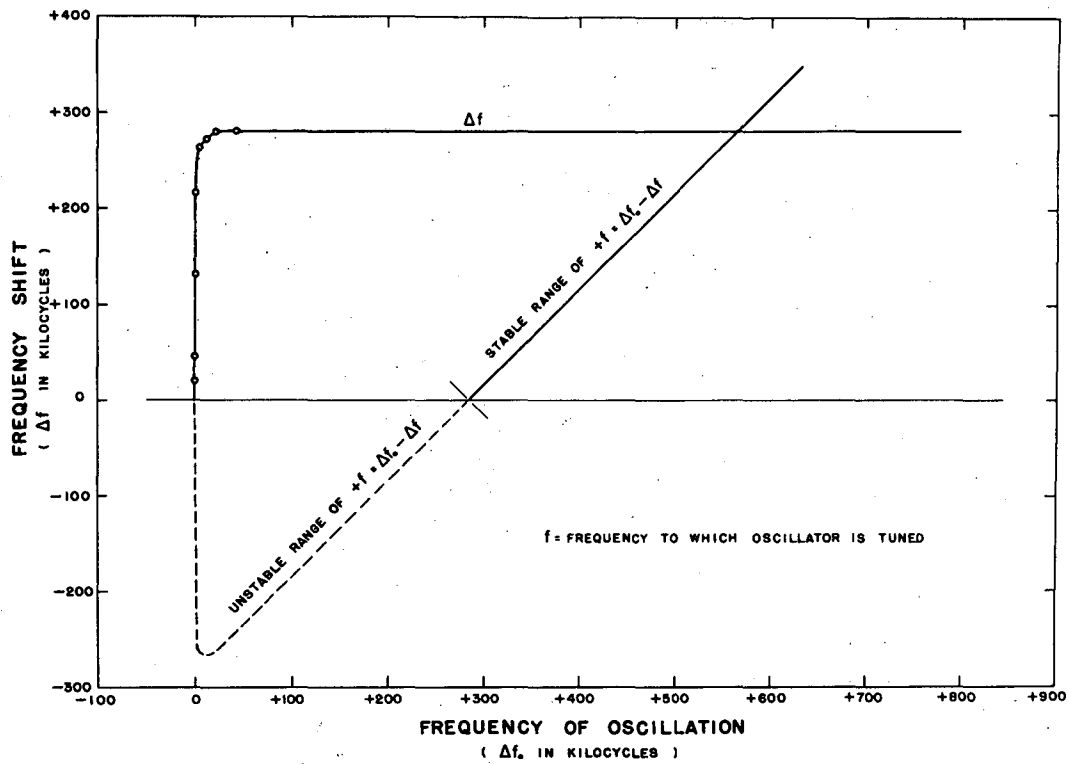


Fig. 12. Case II: Frequency of oscillation and power output as functions of the frequency to which the oscillator is tuned.



MU-10215

Fig. 13. Case II: Relation between frequency of oscillation and frequency shift (lower frequencies).



MU-10216

Fig. 14. Case II: Relation between frequency of oscillation and frequency shift (higher frequencies).

C. Case III

Case III is solved by using graphical calculators No. 1, No. 2, and No. 3. It differs from Cases I and II only by the nature of the feedback network and the phase of the feedback voltage, V_{fb} . The feedback-coupling impedance Z_c is a pure resistance instead of a capacitor, as in Cases I and II. The feedback voltage is in phase with the grid voltage, and as a result the feedback-coupling system is greatly simplified. The circuit values below can be identified by referring to Figs. 5, 6, and 7.

$$Z_c = 5000 \text{ ohms (resistance)}$$

$$Z_1 = \infty$$

$$Z_2 = \infty$$

$$Z_3 = 0$$

$$h = 0.707$$

$$c = 1.0 / 0^\circ$$

$$\frac{Z_{011}}{Z_{01}} = 4.4$$

$$Z_{01}$$

$$\frac{A_{l2}}{A_{l1}} = 0.364$$

$$A_{l1}$$

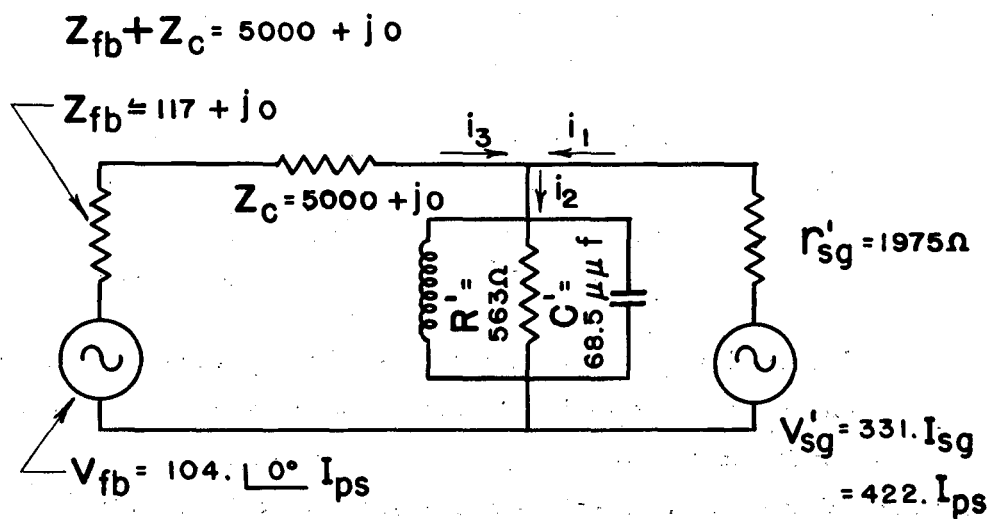
The equivalent circuit for Case III is shown in Fig. 15.

The power output is dependent only on the characteristics of the load impedance and the frequency of oscillation, since the tube acts essentially as a constant-current generator (see p. 9). The operating point of the tube and the load impedance are the same as in Cases I and II and therefore the power output as a function of frequency is again given by Table III.

The relative magnitudes of the feedback and grid voltages are the same as in the two previous cases and are given by Eq. (30).

$$\left| \frac{V_{fb}}{V'_{rs}} \right| = \frac{104.}{93.6} = 1.11 \quad (34)$$

The normalizing constant can be evaluated by first calculating the feedback current at the natural resonant frequency of the load:



MU-10217

Fig. 15. Equivalent circuit for Case III.

$$\begin{aligned}
 i_3 &= \frac{V'_{rs} - V_{fb}}{Z_{fb} + Z_c} = \frac{93.6 I_{ps} - V_{fb}}{5000} \\
 &= \left[93.6 I_{ps} \angle 104^\circ - 104^\circ I_{ps} \right] \left[2.0 \times 10^{-4} \right] \\
 &= 20.8 \times 10^{-4} I_{ps}
 \end{aligned} \tag{35}$$

The normalizing constant is

$$N = \frac{20.8 \times 10^{-4}}{0.11} = 189. \times 10^{-4} \tag{36}$$

The equivalent shunt capacity C'' is again found by using Eq. (33).

The value of C''' is found as in Case I, and the Δf is again obtained by use of Eq. (28). (see p. 26).

The results as obtained by use of the graphical calculators are tabulated in Table V, and are plotted in Fig. 16, as obtained with the aid of Fig. 17.

D. Case IV

Case IV differs from Case I only in that the feedback voltage V_{fb} leads the grid voltage V'_{rs} by the same phase angle as that by which in Case I it lagged the grid voltage. The feedback-coupling impedance Z_c is an inductance. The circuit values below can be identified by referring to Figs. 5, 6, and 7.

$$\begin{aligned}
 Z_c &= j330. \text{ (} 0.259 \times 10^{-6} \text{ henry)} \\
 Z_1 &= j37,300 \text{ (} 29.3 \times 10^{-6} \text{ henry)} \\
 Z_2 &= 10,000 \text{ ohms resistance} \\
 Z_3 &= -j5000 \text{ (} 0.157 \times 10^{-12} \text{ farad)} \\
 h &= 0.707 \\
 c &= 1.0 / +30^\circ \\
 \frac{Z_{011}}{Z_{01}} &= 4.4 \\
 \frac{A_{l2}}{A_{l1}} &= 0.364
 \end{aligned}$$

Table V

Case III. Frequency shift as a function of the frequency of oscillation

Δf_0 (cps)	$i_3 \times 1/N$ (amp)	$i_3 \times 1/N$ (quad. part) (amp)	i_3 (quad. part) (amp)	C'' (μmf)	C''' (μmf)	Δf (kc)
0	$0.11 / -180.0^\circ I_{ps}$	0	0	0	$C''' = C''$	0
+470	$0.33 / +88.5^\circ I_{ps}$	$0.33 / +90^\circ I_{ps}$	$+62.4 \times 10^{-4} / +90^\circ I_{ps}$	+0.052	$C''' = C''$	-77.0
-470	$0.33 / -88.5^\circ I_{ps}$	$0.33 / -90^\circ I_{ps}$	$-62.4 \times 10^{-4} / +90^\circ I_{ps}$	-0.052	$C''' = C''$	+77.0
+705	$0.46 / +74.5^\circ I_{ps}$	$0.44 / +90^\circ I_{ps}$	$+83.2 \times 10^{-4} / +90^\circ I_{ps}$	+0.070	$C''' = C''$	-104.
-705	$0.46 / -74.5^\circ I_{ps}$	$0.44 / -90^\circ I_{ps}$	$-83.2 \times 10^{-4} / +90^\circ I_{ps}$	-0.070	$C''' = C''$	+104.
+1410	$0.71 / +50.5^\circ I_{ps}$	$0.55 / +90^\circ I_{ps}$	$+104. \times 10^{-4} / +90^\circ I_{ps}$	+0.087	$C''' = C''$	-129.
-1410	$0.71 / -50.5^\circ I_{ps}$	$0.55 / -90^\circ I_{ps}$	$-104. \times 10^{-4} / +90^\circ I_{ps}$	-0.087	$C''' = C''$	+129.
+2820	$0.89 / +29.0^\circ I_{ps}$	$0.43 / +90^\circ I_{ps}$	$+81.3 \times 10^{-4} / +90^\circ I_{ps}$	+0.068	$C''' = C''$	-100.
-2820	$0.89 / -29.0^\circ I_{ps}$	$0.43 / -90^\circ I_{ps}$	$-81.3 \times 10^{-4} / +90^\circ I_{ps}$	-0.068	$C''' = C''$	+100.
+5640	$0.97 / +14.8^\circ I_{ps}$	$0.25 / +90^\circ I_{ps}$	$+46.3 \times 10^{-4} / +90^\circ I_{ps}$	+0.039	$C''' = C''$	-57.7
-5640	$0.97 / -14.8^\circ I_{ps}$	$0.25 / -90^\circ I_{ps}$	$-46.3 \times 10^{-4} / +90^\circ I_{ps}$	-0.039	$C''' = C''$	+57.7
+11280	$0.99 / + 7.5^\circ I_{ps}$	$0.13 / +90^\circ I_{ps}$	$+23.6 \times 10^{-4} / +90^\circ I_{ps}$	+0.020	$C''' = C''$	-29.6
-11280	$0.99 / - 7.5^\circ I_{ps}$	$0.13 / -90^\circ I_{ps}$	$-23.6 \times 10^{-4} / +90^\circ I_{ps}$	-0.020	$C''' = C''$	+29.6
+22560	$0.99 / + 4.0^\circ I_{ps}$	$0.03 / +90^\circ I_{ps}$	$+ 5.9 \times 10^{-4} / +90^\circ I_{ps}$	+0.005	$C''' = C''$	- 7.4
-22560	$0.99 / - 4.0^\circ I_{ps}$	$0.03 / -90^\circ I_{ps}$	$- 5.9 \times 10^{-4} / +90^\circ I_{ps}$	-0.005	$C''' = C''$	+ 7.4
+45120	$0.99 / + 2.0^\circ I_{ps}$	$0.02 / +90^\circ I_{ps}$	$+ 2.8 \times 10^{-4} / +90^\circ I_{ps}$	+0.002	$C''' = C''$	- 3.0
-45120	$0.99 / - 2.0^\circ I_{ps}$	$0.02 / -90^\circ I_{ps}$	$- 2.8 \times 10^{-4} / +90^\circ I_{ps}$	-0.002	$C''' = C''$	+ 3.0

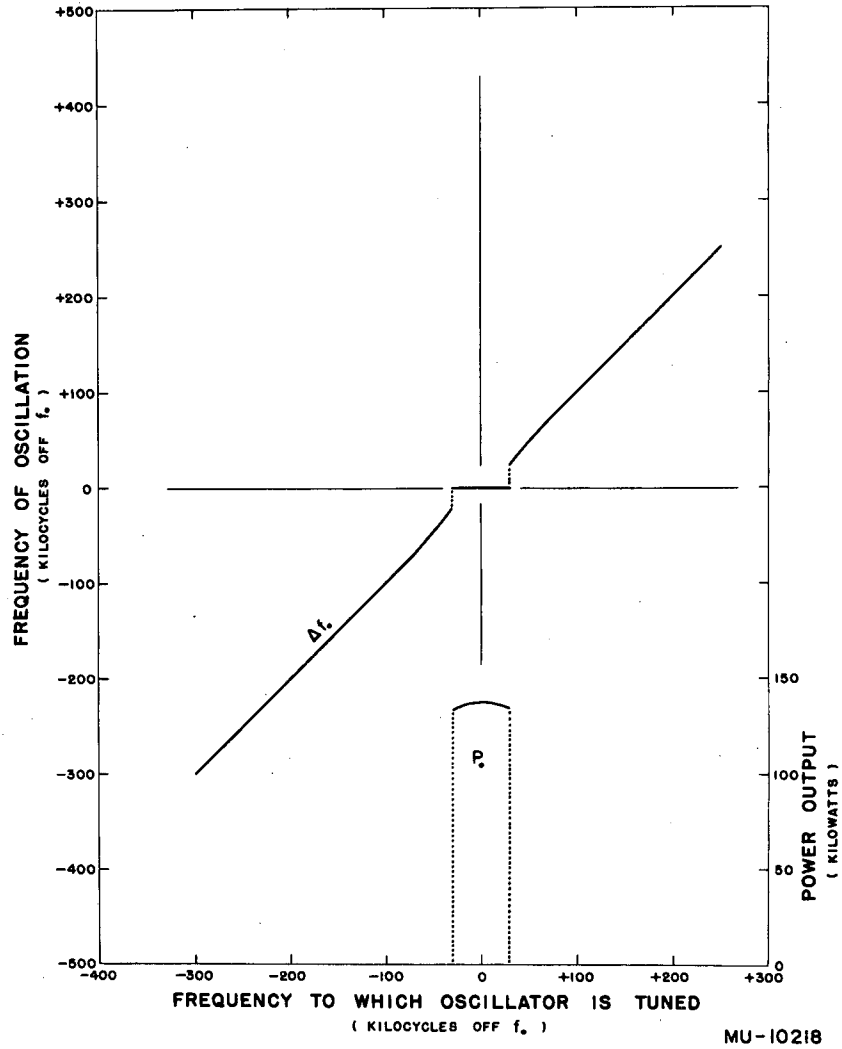


Fig. 16. Case III: Frequency of oscillation and power output as functions of the frequency to which the oscillator is tuned.

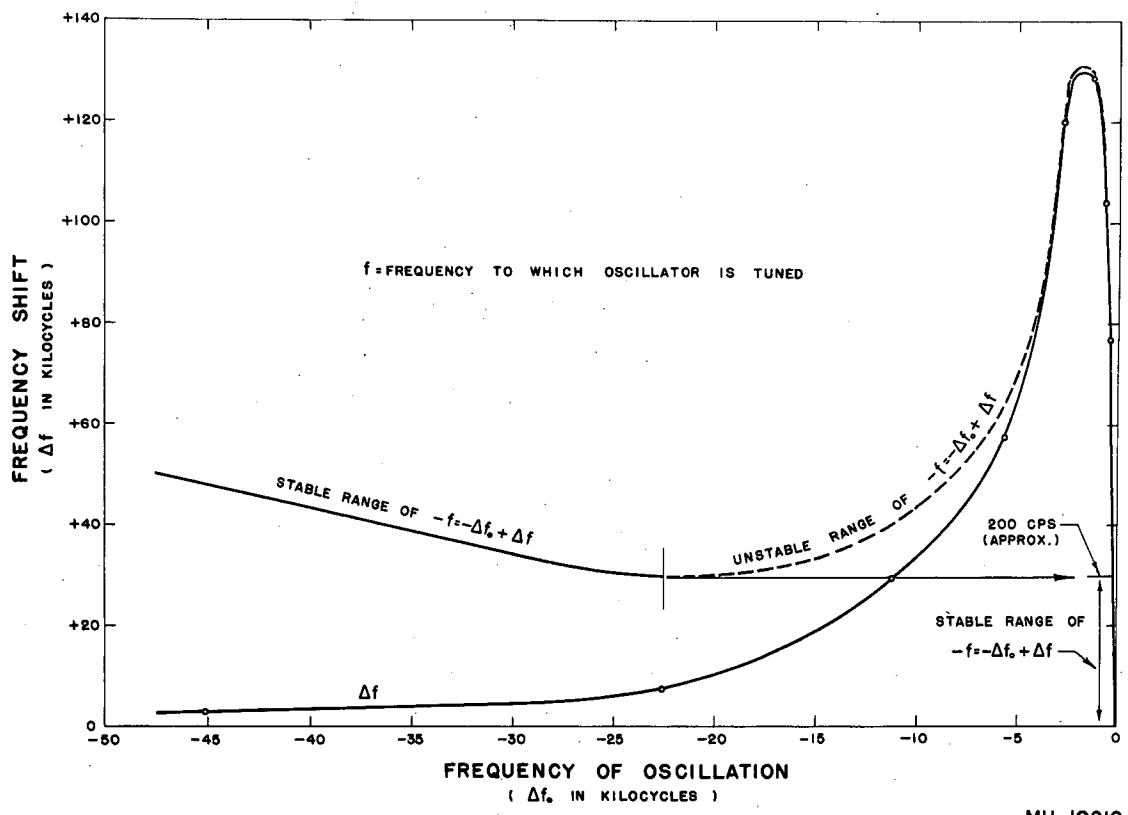


Fig. 17. Case III: Relation between frequency of oscillation and frequency shift.

The equivalent circuit for Case IV is shown in Fig. 18.

The power output, as in all previous cases (see p. 37), is obtained by the use of Table III.

The relative magnitudes of the feedback and grid voltages are the same as in all previous cases and are given by Eqs. (30) and (34):

$$\left| \frac{V_{fb}}{V'_{rs}} \right| = \frac{104.}{93.6} = 1.11 \dots \quad (37)$$

The normalizing constant can be evaluated by first calculating the feedback current at the natural resonant frequency of the load, as in Eqs. (25) and (26):

$$\begin{aligned} i_3 &= \frac{V'_{rs} - V_{fb}}{Z_{fb} + Z_c} = \frac{93.6 I_{ps} - V_{fb}}{2500 - j4000} \\ &= \left[93.6 I_{ps} - 104. / +30^\circ I_{ps} \right] \left[1.12 - j1.80 \right] 10^{-4} \\ &= \left[97.4 - j52.2 \right] 10^{-4} I_{ps} \end{aligned} \quad (38)$$

In the above calculation the value of Z_{fb} is found to be the conjugate of the Z_{fb} of Case I, pgs. 21 and 23.

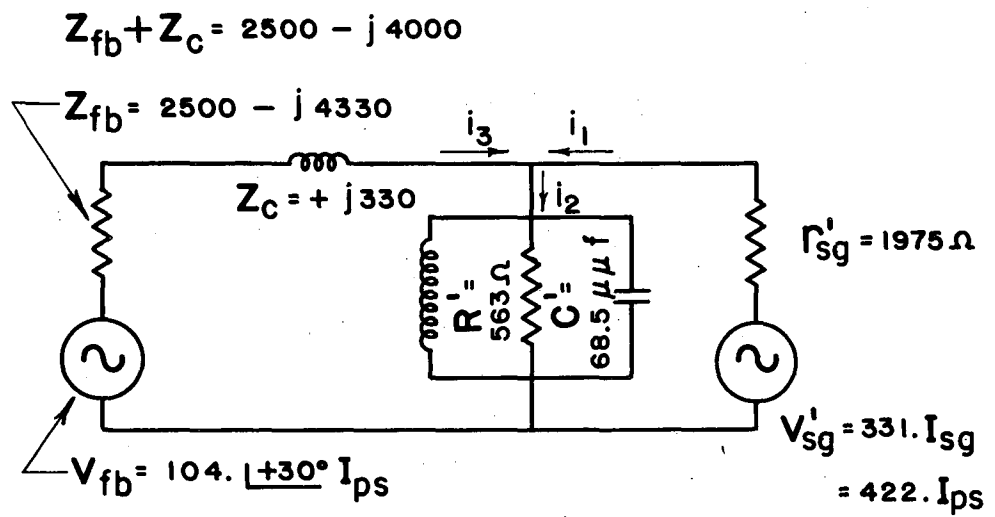
The normalizing constant is

$$N = \frac{52.2 \times 10^{-4}}{0.21} = 248 \times 10^{-4} \quad (39)$$

The equivalent shunt capacity C'' is found by using Eq. (33).

The value of C'' is found as in Case I page 26, and the Δf is again obtained by use of Eq. (28).

The results as obtained by use of the graphical calculators are tabulated in Table VI, and are plotted in Fig. 19, as obtained with the aid of Figs. 20 and 21.



MU-10220

Fig. 18. Equivalent circuit for case IV.

Table VI

Case IV. Frequency shift as a function of the frequency of oscillation

Δf_0 (cps)	$i_3 \times 1/N$ (amp)	$i_3 \times 1/N$ (quad. part), (amp)	i_3 (quad. part) (amp)	C'' (μmf)	C''' (μmf)	Δf (kc)
0	0.47/ <u>-27.0</u> ^o I _{ps}	0.21/ <u>-90</u> ^o I _{ps}	-52.2 x 10 ⁻⁴ / <u>+90</u> ^o I _{ps}	-0.044	0	0
+470	0.18/ <u>+39.5</u> ^o I _{ps}	0.12/ <u>-90</u> ^o I _{ps}	-29.8 x 10 ⁻⁴ / <u>+90</u> ^o I _{ps}	-0.025	+0.019	-27.5
-470	0.71/ <u>+11.0</u> ^o I _{ps}	0.14/ <u>-90</u> ^o I _{ps}	-34.8 x 10 ⁻⁴ / <u>+90</u> ^o I _{ps}	-0.029	+0.015	-21.8
+705	0.05/ <u>-12.7</u> ^o I _{ps}	0.01/ <u>-90</u> ^o I _{ps}	- 2.5 x 10 ⁻⁴ / <u>+90</u> ^o I _{ps}	-0.002	+0.042	-62.3
-709	0.80/ <u>- 3.5</u> ^o I _{ps}	0.05/ <u>-90</u> ^o I _{ps}	-12.4 x 10 ⁻⁴ / <u>+90</u> ^o I _{ps}	-0.010	+0.033	-49.3
+1410	0.27/ <u>+98.0</u> ^o I _{ps}	0.26/ <u>+90</u> ^o I _{ps}	+64.5 x 10 ⁻⁴ / <u>+90</u> ^o I _{ps}	+0.050	+0.099	-145.
-1410	0.93/ <u>+14.5</u> ^o I _{ps}	0.23/ <u>+90</u> ^o I _{ps}	+57.1 x 10 ⁻⁴ / <u>+90</u> ^o I _{ps}	+0.048	+0.091	-135.
+2820	0.55/ <u>+82.5</u> ^o I _{ps}	0.54/ <u>+90</u> ^o I _{ps}	+134. x 10 ⁻⁴ / <u>+90</u> ^o I _{ps}	+0.113	+0.157	-232.
-2820	0.97/ <u>+32.5</u> ^o I _{ps}	0.51/ <u>+90</u> ^o I _{ps}	+127. x 10 ⁻⁴ / <u>+90</u> ^o I _{ps}	+0.106	+0.149	-220.
+5640	0.71/ <u>+71.0</u> ^o I _{ps}	0.68/ <u>+90</u> ^o I _{ps}	+169. x 10 ⁻⁴ / <u>+90</u> ^o I _{ps}	+0.142	+0.186	-276.
-5640	0.93/ <u>+44.5</u> ^o I _{ps}	0.66/ <u>+90</u> ^o I _{ps}	+164. x 10 ⁻⁴ / <u>+90</u> ^o I _{ps}	+0.138	+0.181	-268.
+11280	0.78/ <u>+64.0</u> ^o I _{ps}	0.70/ <u>+90</u> ^o I _{ps}	+174. x 10 ⁻⁴ / <u>+90</u> ^o I _{ps}	+0.146	+0.191	-283.
-11280	0.89/ <u>+51.0</u> ^o I _{ps}	0.69/ <u>+90</u> ^o I _{ps}	+171. x 10 ⁻⁴ / <u>+90</u> ^o I _{ps}	+0.144	+0.187	-276.
+22560	0.82/ <u>+61.0</u> ^o I _{ps}	0.72/ <u>+90</u> ^o I _{ps}	+179. x 10 ⁻⁴ / <u>+90</u> ^o I _{ps}	+0.149	+0.193	-283.
-22560	0.87/ <u>+54.5</u> ^o I _{ps}	0.70/ <u>+90</u> ^o I _{ps}	+174. x 10 ⁻⁴ / <u>+90</u> ^o I _{ps}	+0.146	+0.191	-283.
+45120	0.83/ <u>+59.5</u> ^o I _{ps}	0.72/ <u>+90</u> ^o I _{ps}	+179. x 10 ⁻⁴ / <u>+90</u> ^o I _{ps}	+0.149	+0.193	-283.
-45120	0.86/ <u>+56.5</u> ^o I _{ps}	0.71/ <u>+90</u> ^o I _{ps}	+176. x 10 ⁻⁴ / <u>+90</u> ^o I _{ps}	-0.148	+0.191	-283.

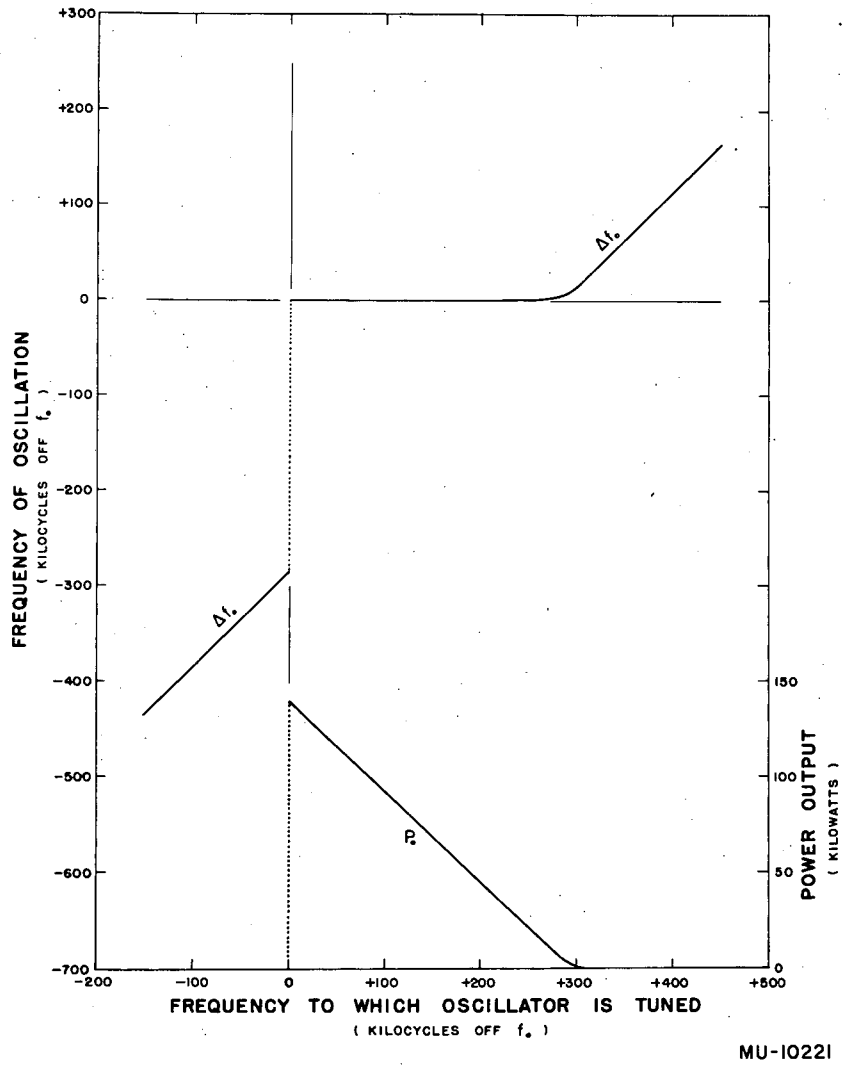
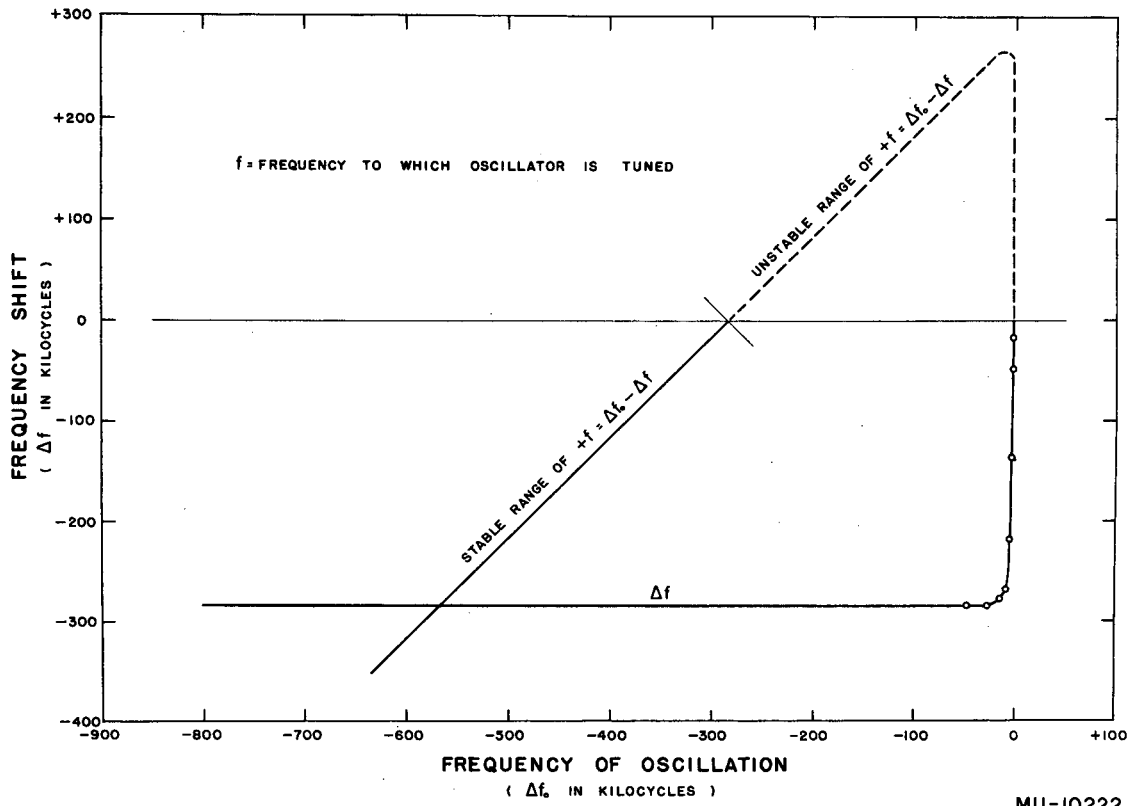


Fig. 19. Case IV: Frequency of oscillation and power output as functions of the frequency to which the oscillator is tuned.



MU-10222

Fig. 20. Relation between frequency of oscillation and frequency shift (lower frequencies).

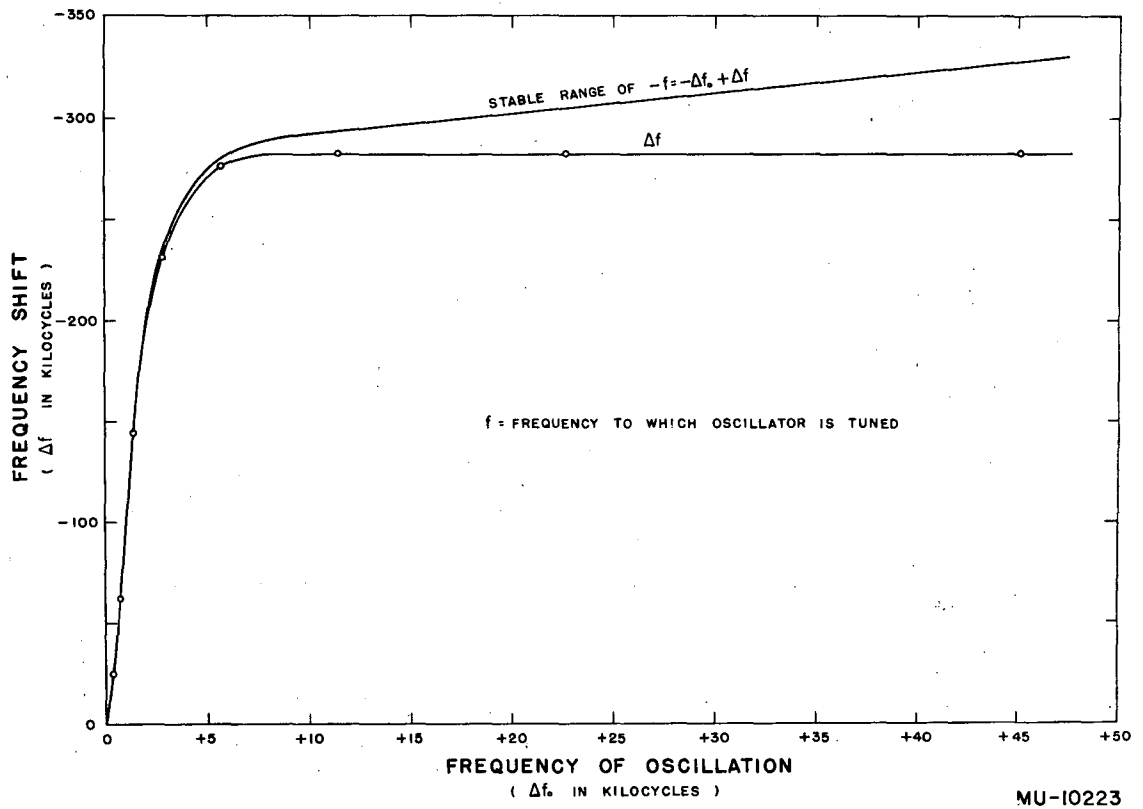


Fig. 21. Relation between frequency of oscillation and frequency shift (higher frequencies).

IV. CONCLUSIONS

This oscillator is a stabilized oscillator and not a synchronized oscillator such as has been studied by Adler,¹ Appleton,⁴ Huntoon,⁵ and others. However, it does exhibit characteristics strikingly similar to the "locking" of a synchronized oscillator, particularly in the resistance feedback-coupling impedance of Case III (p. 37).

The "pulling bandwidth" with the resistance feedback-coupling impedance was narrower than with the reactive coupling, although approximately the same voltage and circuit impedances were used in all cases. The oscillating frequency, in a compensating way, was very much closer to the natural frequency of the load and the power output was very constant over the narrower bandwidth.

The jump in the experimental curve B, (see Fig. 27 in Appendix F) was identified as an accidental resonance in the grid circuit at the time the experimental data were taken. This effect can be eliminated by properly adjusting the circuit parameters in the grid circuit.

The unstable regions indicated in Figs. 11, 14, 16, and 19 follow reasonably from the fact that the feedback changes the frequency during the buildup of oscillations in the resonant load, and the final equilibrium frequency will be the first stable situation found by the oscillator. This frequency modulation has been observed but not measured.

This work was done under the auspices of the U. S. Atomic Energy Commission.

V. APPENDICES

A. Calculation for the Q of the Cathode-Grid-Screen Circuit

The following calculations are based on physical measurements of the oscillator and the operating conditions of the tube. The voltages and the dimensions of the cathode-grid-screen circuit are both shown in Fig. 22.

A fundamental definition of Q^7 is

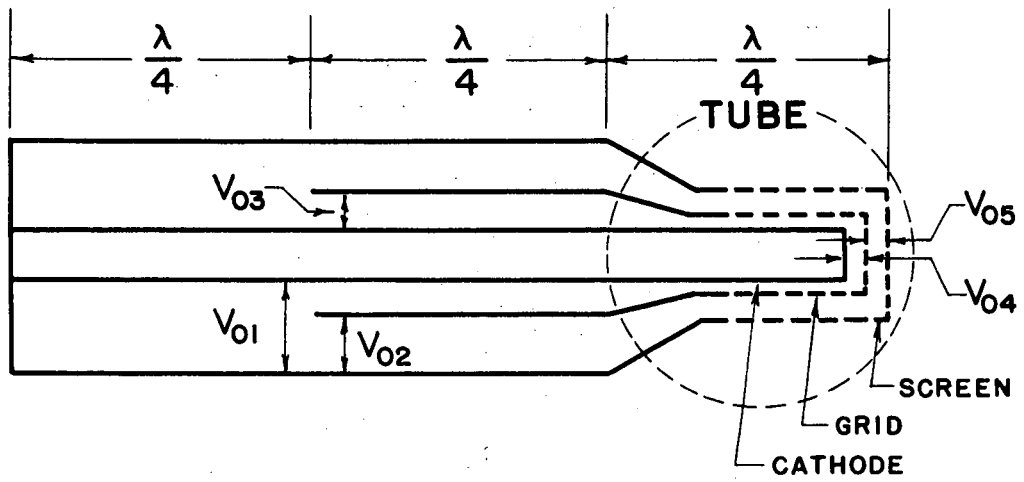
$$Q = \frac{2\pi \text{ energy stored at peak of cycle}}{\text{energy dissipated per cycle}}$$
$$= \frac{\omega \text{ energy stored at peak of cycle}}{\text{power dissipated}}$$

The Q of this grid circuit, which is composed of several transmission lines tightly coupled together, is

$$Q = \frac{\omega [W_{s1} + W_{s2} + \dots + W_{s5}]}{[W_{d1} + W_{d2} + \dots + W_{d5}]}$$

The energy stored per quarter wavelength of coaxial transmission line is calculated first. Since the circuit losses are small when large brass conductors are used, the voltage and current distributions are nearly sinusoidal. A small error is introduced in the calculations if they are assumed to be exactly sinusoidal. We have

$$\Delta W_s = \frac{\Delta C_o V^2}{2}, \quad \Delta C_o = C_o \Delta l,$$
$$\Delta W_s = \frac{C_o \Delta l V^2}{2},$$



MU-10225

Fig. 22. Cathode-grid-screen circuit.

$$\begin{aligned} \int_0^{W_s} dW_s &= \frac{\lambda C_o V_0^2}{4\pi} \int_0^{\pi/2} \sin^2 \left(\frac{2\pi \ell}{\lambda} \right) d \left(\frac{2\pi \ell}{\lambda} \right) \\ &= \frac{\lambda C_o V_0^2}{4\pi} \left[\frac{1}{2} \left(\frac{2\pi \ell}{\lambda} \right) - \frac{1}{4} \sin 2 \left(\frac{2\pi \ell}{\lambda} \right) \right] \\ W_s &= \frac{\lambda C_o V_0^2}{16} \end{aligned}$$

The energy dissipated per quarter wavelength of coaxial transmission line is as follows.

$$\begin{aligned} I &= I_0 \cos \left(\frac{2\pi \ell}{\lambda} \right), \\ \Delta W_d &= \frac{\Delta R I^2}{2}, \quad \Delta R = R \Delta \ell, \\ \Delta W_d &= \frac{R \Delta \ell I^2}{2}, \\ \int_0^{W_d} dW_d &= \frac{\lambda R I_0^2}{4\pi} \int_0^{\pi/2} \cos^2 \left(\frac{2\pi \ell}{\lambda} \right) d \left(\frac{2\pi \ell}{\lambda} \right), \\ W_d &= \frac{\lambda R I_0^2}{4\pi} \left[\frac{1}{2} \left(\frac{2\pi \ell}{\lambda} \right) + \frac{1}{4} \sin 2 \left(\frac{2\pi \ell}{\lambda} \right) \right], \\ W_d &= \frac{\lambda R I_0^2}{16} \end{aligned}$$

For both conductors of a coaxial transmission line,

$$W_d = \frac{\lambda I_0^2}{16} [R_i + R_o], \quad R_i = \frac{r_{si}}{\pi d_i}, \quad R_o = \frac{r_{so}}{\pi d_o}$$

If the inner and outer conductors are of the same material,

$$[R_i + R_o] = \frac{r_s}{2\pi} \left[\frac{2}{d_i} + \frac{2}{d_o} \right],$$

$$W_d = \frac{\lambda r_s I_0^2}{32\pi} \left[\frac{2}{d_i} + \frac{2}{d_o} \right].$$

The total Q of the composite system is

$$Q_t = \frac{\left(\frac{\omega\lambda}{16}\right) [C_{o1} V_{01}^2 + C_{o2} V_{02}^2 + \dots + C_{o5} V_{05}^2]}{\left(\frac{\lambda r_s}{32\pi}\right) \left[I_{01}^2 \left(\frac{2}{d_{i1}} + \frac{2}{d_{o1}} \right) + I_{02}^2 \left(\frac{2}{d_{i2}} + \frac{2}{d_{o2}} \right) + \dots + I_{05}^2 \left(\frac{2}{d_{i5}} + \frac{2}{d_{o5}} \right) \right]}$$

Assuming sinusoidal distributions of voltage and current in a quarter wavelength resonant transmission line, we find the relation

$$V_0 = I_0 Z_0.$$

The composite Q is then

$$Q_t = \frac{2\pi\omega}{r_s} \frac{[C_{o1} V_{01}^2 + C_{o2} V_{02}^2 + \dots + C_{o5} V_{05}^2]}{\left[\frac{V_{01}^2}{Z_{01}^2} \left(\frac{2}{d_{i1}} + \frac{2}{d_{o1}} \right) + \frac{V_{02}^2}{Z_{02}^2} \left(\frac{2}{d_{i2}} + \frac{2}{d_{o2}} \right) + \dots + \frac{V_{05}^2}{Z_{05}^2} \left(\frac{2}{d_{i5}} + \frac{2}{d_{o5}} \right) \right]}$$

The characteristic impedance (Z_0) of a coaxial transmission line is given by

$$Z_0 = 138 \log_{10} \left(\frac{d_o}{d_i} \right) \text{ ohms.}$$

With the aid of the above relation and the physical dimensions of the oscillator, the characteristic impedances of the transmission lines in the cathode-grid-screen circuit have been calculated. These are listed in Table VII. The relative voltages are based on the tube calculations in Appendix B (p. 56), and are given in Table VII in terms of V_{02} for the condition that $V_{04} = 0.796 V_{05}$.

Table VII

Open-end voltage of the several transmission lines
in terms of the open-end voltage of Line 2

Trans. Line No.	$\frac{d_o}{Z}$ (m)	$\frac{d_i}{Z}$ (m)	$\frac{d_o}{d_i}$	$\frac{2}{d_i}$	$\frac{2}{d_o}$	$\frac{2}{d_i} + \frac{2}{d_o}$	$\log \frac{d_o}{d_i}$	Z_0 (ohms)	Voltage
1	0.089	0.038	2.34	26.3	11.2	37.5	0.369	51.0	$V_{01} = 0.497V_{02}$
2	0.089	0.057	1.56	17.5	11.2	28.7	0.193	26.6	$V_{02} = V_2$
3	0.057	0.047	1.21	21.3	17.5	38.8	0.083	11.5	$V_{03} = 0.503V_{02}$
4	0.028	0.023	1.22	43.4	35.7	79.1	0.088	12.2	$V_{04} = 0.532V_{02}$
5	0.038	0.028	1.34	35.7	26.3	62.0	0.129	17.7	$V_{05} = 0.667V_{02}$

By using the relation ⁷

$$C_o = \frac{0.241 \epsilon_1}{\log_{10} \left(\frac{d_o}{d_i} \right)} 10^{-10} \text{ farad per meter,}$$

we get the final expression for Q_t :

$$Q_t = \frac{0.48 \omega \pi \epsilon_1 10^{-10} \left[\frac{V_{01}^2}{\log \left(\frac{d_{o1}}{d_{i1}} \right)} + \frac{V_{02}^2}{\log \left(\frac{d_{o2}}{d_{i2}} \right)} + \dots + \frac{V_{05}^2}{\log \left(\frac{d_{o5}}{d_{i5}} \right)} \right]}{r_s \left[\frac{V_{01}^2}{Z_{01}^2} \left(\frac{2}{d_{i1}} + \frac{2}{d_{o1}} \right) + \frac{V_{02}^2}{Z_{02}^2} \left(\frac{2}{d_{i2}} + \frac{2}{d_{o2}} \right) + \dots + \frac{V_{05}^2}{Z_{05}^2} \left(\frac{2}{d_{i5}} + \frac{2}{d_{o5}} \right) \right]}$$

$$Q_t = \frac{0.482 \omega \pi \epsilon_1 10^{-10} [0.670 + 5.19 + 3.05 + 3.22 + 3.45]}{r_s [0.003 + 0.041 + 0.074 + 0.152 + 0.088]}$$

$$Q_t = \frac{0.482 \omega \pi \epsilon_1 10^{-10}}{r_s} \left[\frac{15.6}{0.358} \right].$$

The surface resistivity of brass⁶ is

$$r_s = 5.01 \times 10^{-7} \sqrt{f} \text{ ohm per square.}$$

This gives, for the total Q,

$$Q_t = \frac{0.482 \times 2\pi \times 202.55 \times 10^6 \times \pi \times 10^{-10}}{5.01 \times 10^{-7} \sqrt{202.55 \times 10^6}} [43.6],$$

$$Q_t = 1170 \text{ (measured value}^* \text{ } Q_m = 570).$$

The ratio of the calculated Q to the measured Q gives the ratio of the actual conductor losses to the calculated losses. The stored energy is the same in either case. We find

$$\frac{Q_c}{Q_m} = \frac{W_{dm}}{W_{dc}} = \frac{1170}{570} = 2.06.$$

The effect of the grid drive power is to further lower the Q by adding an additional loss in the circuit. From Appendix B, the grid drive power is

$$\begin{aligned} P_g &= I_g V_g \text{ (crest value)} \\ &= 5.2 (600 + 1200) \\ &= 9340 \text{ watts} \end{aligned}$$

$$R_g = \frac{V_g^2}{2P_g} = \frac{1800^2}{2 \times 9340} = 174 \text{ ohms}$$

Since the grid drive power is dissipated at the open end of transmission line No. 4, it may be included in the expression for Q_t by writing the expression in the form

$$W_g = \frac{V_{04}^2}{2R_g} = \frac{[0.532 V_{02}]^2}{2 \times 174} = 8.14 \times 10^{-4} V_{02}^2$$

* see Appendix F.

and normalizing,

$$W_g = \frac{32\pi}{\lambda r_s} \times 8.14 \times 10^{-4} V_{02}^2 = 7.75 V_{02}^2$$

The corrected value of Q_t including the grid drive power is

$$Q_t = 1170 \times \frac{1}{43.6} \left[\frac{15.6}{0.358 \times 1.97 + 7.75} \right]$$

$$= \left[\frac{1170}{43.6} \right] \left[\frac{15.6}{8.49} \right]$$

$$Q_t = 49.2$$

B. Calculation of Tube Operation

The function of the oscillating cathode-grid-screen circuit is to supply the maximum fundamental component of space current to the output (anode) circuit. An operating point for the tube must be chosen that insures strong self-oscillation. Since the maximum possible current is to flow to the anode, the efficiency must be as low as possible consistent with strong self-oscillation. As is shown in the analysis, the following operating point for the tube fits these requirements:

$$\begin{aligned} E_p &= 10,000 \text{ volts dc} \\ E_s &= 3,000 \text{ volts dc} \\ E_g &= 600 \text{ volts dc} \\ e_{gm} &= 1,200 \text{ volts (instantaneous)} \\ e_{pm} &= 5,420 \text{ volts (instantaneous)} \\ e_{sm} &= 2,540 \text{ volts (instantaneous)} \\ V_{pc} &= E_p - e_{pm} = 4,580 \text{ volts ac} \\ V_{sc} &= E_s - e_{sm} = 460 \text{ volts ac} \end{aligned}$$

Since it is assumed that e_{gm} , e_{pm} , and e_{sm} go through their crest values at the same time, the graphical Fourier analysis for the

case of a symmetrical wave shape can be used. This has been worked out in Appendix C (pg. 64).

For the above operating point, the electrode voltages and currents corresponding to the graphical analysis points are tabulated in Table VIII. These points are also plotted on the load lines for the tube (4W20,000A) in Fig.23. On examination of the values of the currents at each of the analysis points we note that only F(0) through F(6) contribute, and all others beyond F(6) are zero.

The dc value of the grid current is calculated by using the relation from Appendix C (p. 64):

$$\begin{aligned} I_g &= \frac{1}{12} [0.5 F(0) + F(1) + F(2) + \dots + F(23) + 0.5 F(24)] \\ &= \frac{1}{12} [0.5 \times 23.5 + 22.5 + 17.4 + 10.2 + 0.38 + 0.0] \\ &= \frac{1}{12} [62.2] = 5.2 \text{ amperes} \end{aligned}$$

The screen currents are calculated by using the relations in Appendix C (pg. 64):

$$\begin{aligned} I_{sg} &= \frac{1}{12} [F(0) + 1.93F(1) + 1.73F(2) + 1.41F(3) + F(4) + 0.518F(5)] \\ &= \frac{1}{12} [139 + 1.93 \times 139 + 1.73 \times 126 + 1.41 \times 105 + 63.4 + 0.518 \times 11.1] \\ &= \frac{1}{12} [842] = 70.1 \text{ amperes (crest value of fundamental component).} \\ I_s &= \frac{1}{12} [0.5 \times 39.0 + 37.5 + 27.0 + 14.3 + 2.4 + 0.4] \\ &= \frac{1}{12} 101.1 = 8.4 \text{ amperes (dc value).} \end{aligned}$$

Table VIII

Electrode voltages and currents corresponding to graphical analysis points

	θ	$\cos \theta$	e_g (volts)	e_s (volts)	e_p (volts)	i_g (amps)	i_s (amps)	i_p (amps)
F(0)	0°	1.00	1200	2540	5420	23.5	39.0	100.
F(1)	15°	.996	1138	2556	5570	22.5	37.5	101.
F(2)	30°	.886	950	2600	6030	17.4	27.0	99.
F(3)	45°	.707	670	2680	6760	10.2	14.3	91.
F(4)	60°	.500	300	2770	7710	.38	2.4	61
F(5)	75°	.259	-133	2880	8810	0	.4	10.7
F(6)	90°	.000	-600	3000	10000	0	0	0

The plate currents are calculated by using the same relations:

$$I_{ps} = \frac{1}{12} [100 + 1.93 \times 101 + 1.73 \times 99.0 + 1.41 \times 91.0 + 61.0 + 0.518 \times 10.7]$$

$$= \frac{1}{12} [661] = 55.0 \text{ amperes (crest value of the fundamental component).}$$

$$I_p = \frac{1}{12} [0.5 \times 100 + 101 + 99.0 + 91.0 + 61.0 + 10.7]$$

$$= \frac{1}{12} [413] = 34.4 \text{ amperes (dc value).}$$

The power output is the product of the fundamental components of plate current and plate-to-screen voltage:

$$P_o = \frac{I_{ps}}{\sqrt{2}} \frac{V_{ps}}{\sqrt{2}} = 55 \left(\frac{V_{pc} + V_{sc}}{2} \right) = 138 \text{ kilowatts.}$$

The plate-load impedance at the natural resonant frequency (f_0) of the load is the fundamental component of plate-to-screen voltage divided by the plate current:

$$Z_{ps}(f_0) = R_{ps} = \frac{5040}{55} = 91.7 \text{ ohms.}$$

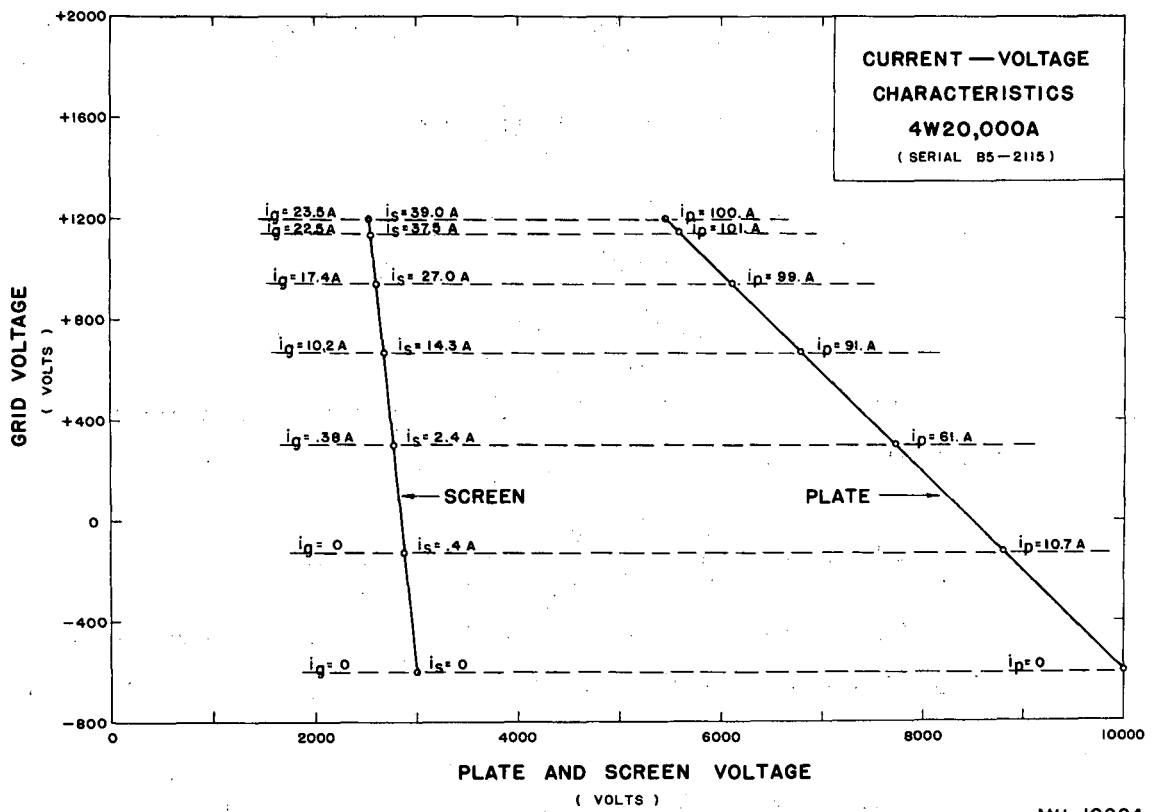


Fig. 23. Current-to-voltage characteristics of 4W20,000A tube (Series B5-2115) at 2750 watts cathode power.

The dc plate power input is the product of the dc plate voltage and dc plate current:

$$\text{Power input} = I_p \times E_p = 34.4 \times 10,000 = 344 \text{ kilowatts.}$$

The plate dissipation is the difference between the plate power input and the plate power output:

$$\text{Plate dissipation} = 344 - 138 = 206 \text{ kilowatts.}$$

The grid drive power can be obtained with sufficient accuracy by using the following relation:⁷

$$\begin{aligned} P_g &= I_g V_g \text{ (crest value)} \\ &= I_g (E_g + e_{gm}) \\ &= 5.2 (600 + 1200), \end{aligned}$$

$$P_g = 9340 \text{ watts.}$$

The plate efficiency is the ratio of the plate power output to the plate power input:

$$\text{Plate efficiency} = \frac{138}{344} = 40.1 \text{ percent.}$$

The screen dissipation is the difference between the screen dc power input and the power generated by the screen circuit:

$$\begin{aligned} \text{Screen dissipation} &= (E_s I_s) - \left[\frac{V_{sc}}{\sqrt{2}} \frac{I_{sg}}{\sqrt{2}} \left(\frac{I_s}{I_s + I_p} \right) \right] \\ &= (3000 \times 8.4) - \left[\frac{460}{\sqrt{2}} \frac{70.1}{\sqrt{2}} \left(\frac{8.4}{8.4 + 34.4} \right) \right] \\ &= 22.1 \text{ kilowatts.} \end{aligned}$$

The grid dissipation can be approximated by using the following relation:^{8,9}

$$\begin{aligned}\text{Grid dissipation} &= I_g V_g - E_g I_g \\ &= (5.2 \times 1800) - (600 \times 5.2) \\ &= 6.2 \text{ kilowatts} .\end{aligned}$$

C. Graphical Fourier Analysis of Nonsinusoidal Wave Forms

The basis of the Fourier analysis is the assumption that the periodic function $F(t)$ may be written in the form

$$F(t) = \left[\begin{aligned} &a_0 + a_1 \cos (wt) + a_2 \cos (2wt) + \dots + a_n \cos (nwt) \\ &+ b_1 \sin (wt) + b_2 \sin (2wt) + \dots + b_n \sin (nwt) \end{aligned} \right]$$

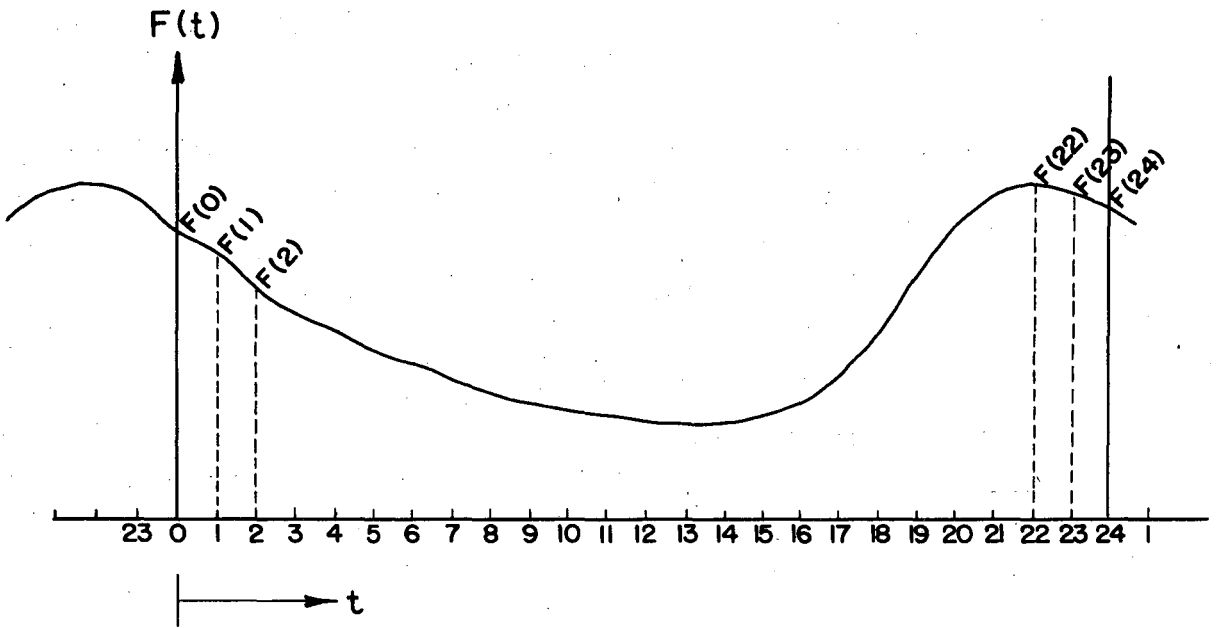
The coefficients in this series can be evaluated as a result of the orthogonality properties of sinusoids. These coefficients have the following forms:⁶

$$a_0 = \frac{1}{2\pi} \int_0^{2\pi} F(t) d(wt) ,$$

$$a_n = \frac{1}{\pi} \int_0^{2\pi} F(t) \cos n(wt) d(wt) ,$$

$$b_n = \frac{1}{\pi} \int_0^{2\pi} F(t) \sin n(wt) d(wt) .$$

For use in a graphical analysis these integrals can be approximated by summations. The wave shape in Fig. 24 can be used as an aid in setting up these summations.



MU-10226

Fig. 24. Arbitrary wave shape used in 24-point analysis.

For a 24-point analysis the sums can be expressed as follows:

$$a = \frac{1}{24} \sum_{m=0}^{m=24} F(m) = \left[\frac{1}{24} \frac{F(0)}{2} + F(1) + F(2) + \dots + \frac{F(24)}{2} \right],$$

$$a_n = \frac{1}{12} \sum_{m=0}^{m=24} F(m) \cos n(m 15^\circ)$$

$$= \frac{1}{12} \left[\frac{F(0) \cos (n 0^\circ)}{2} + F(1) \cos (n 15^\circ) + \dots + \frac{F(24) \cos (n 360^\circ)}{2} \right],$$

$$b_n = \frac{1}{12} \sum_{m=0}^{m=24} F(m) \sin n(m 15^\circ)$$

$$= \frac{1}{12} \left[\frac{F(0) \sin (n 0^\circ)}{2} + F(2) \sin (n 15^\circ) + \dots + \frac{F(24) \sin (n 360^\circ)}{2} \right].$$

For the purpose for which these calculations are to be used, only the fundamental frequency ($n = 1$) is of interest. Summing the terms that have the same numerical coefficients gives the following expressions for a_0 , a_1 , and b_1 :

$$a_0 = \frac{1}{24} \left[\frac{F(0)}{2} + F(1) + F(2) + \dots + \frac{F(24)}{2} \right]$$

$$a_1 = \frac{1}{12} \left\{ \begin{array}{l} [F(0) - F(12)] \cos 0^\circ \\ [F(1) - F(11) + F(23) - F(13)] \cos 15^\circ + \\ [F(2) - F(10) - F(14) + F(22)] \cos 30^\circ + \\ [F(3) - F(9) - F(15) + F(21)] \cos 45^\circ + \\ [F(4) - F(8) - F(16) + F(20)] \cos 60^\circ + \\ [F(5) - F(7) - F(17) + F(19)] \cos 75^\circ + \\ [F(6) - F(18)] \cos 90^\circ \end{array} \right\} ,$$

$$b_1 = \frac{1}{12} \left\{ \begin{array}{l} [F(0) + F(12)] \sin 0^\circ \\ [F(1) + F(11) - F(13) - F(23)] \sin 15^\circ + \\ [F(2) + F(10) - F(14) - F(22)] \sin 30^\circ + \\ [F(3) + F(9) - F(15) - F(21)] \sin 45^\circ + \\ [F(4) + F(8) - F(16) - F(20)] \sin 60^\circ + \\ [F(5) + F(7) - F(17) - F(19)] \sin 75^\circ + \\ [F(6) - F(18)] \sin 90^\circ \end{array} \right\} .$$

For the special case of a wave shape that is symmetrical about $F(0)$, $m = 0$ the sine term is zero ($b_1 = 0$). Also,

$$a_0 = \frac{1}{12} [0.5 F(0) + F(1) + \dots + F(12)] ,$$

$F(0) = F(24)$	$F(4) = F(20)$	$F(8) = F(16)$
$F(1) = F(23)$	$F(5) = F(19)$	$F(9) = F(15)$
$F(2) = F(22)$	$F(6) = F(18)$	$F(10) = F(14)$
$F(3) = F(21)$	$F(7) = F(17)$	$F(11) = F(13)$

$$a_1 = \frac{1}{12} \left\{ \begin{array}{l} [F(0) - F(12) + 1.98 [F(1) - F(11)] \\ + 1.73 [F(2) - F(10)] + 1.41 [F(3) - F(9)] \\ [F(4) - F(8)] + 0.518 [F(5) - F(7)] \end{array} \right\} .$$

D. Calculation of the Plate-Load Impedance
as a Function of Frequency

The universal resonance curves for parallel resonant circuits⁷ have been used to determine the plate-load impedance as a function of frequency. The exact values are fixed by the Q of the resonant load (measured Q = 72,000) and the coupled impedance at resonance. By design, this value has been set at $Z_{ps}(f_0) = R_{ps}(f_0) = 91.7$ ohms. This is calculated in Appendix B.

The plate-load impedance and the resistance component of the plate-load impedance are listed as functions of frequency in Table IX.

E. Proof that the Locus of the Impedance Vector
for a Parallel Circuit is a Circle

In the following proof Q_0 and ω_0 are the Q and the angular frequency at resonance respectively. The proof is concerned with Figs. 25 and 26.

The parallel impedance is as follows:

$$Z = \frac{\left(\frac{j\omega L R}{R + j\omega L}\right)\left(\frac{-j}{\omega C}\right)}{\left(\frac{j\omega L R}{R + j\omega L} - \frac{j}{\omega C}\right)} = \frac{\omega L R}{\omega L - j[R - \omega^2 L R C]}$$

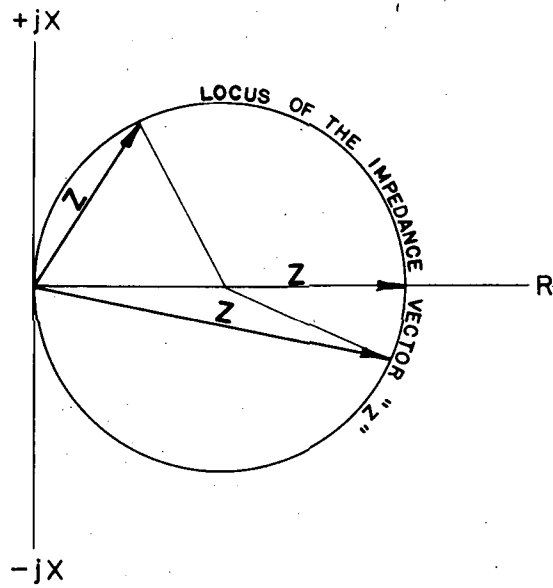
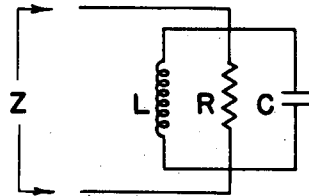
$$= \frac{\omega L}{\frac{\omega L}{R} - j[1 - \omega^2 LC]} = \frac{\omega L \left[\frac{\omega L}{R} + j(1 - \omega^2 LC)\right]}{\frac{\omega^2 L^2}{R^2} + (1 - \omega^2 LC)^2}$$

Now at resonance,

$$LC = \frac{1}{\omega_0^2}$$

Table IX

Plate-load impedance as a function of frequency					
<u>Cycles off resonance</u> <u>resonant frequency</u>	Δf_0 (cps)	<u>Actual impedance</u> <u>impedance at resonance</u>	<u>Phase angle of</u> <u>the impedance</u>	Z_{ps} (ohms)	R_{ps} (ohms)
0	0	1.00	0°	$91.7/0^\circ$	91.7
$\frac{1}{6Q} = \frac{1}{3} \times \frac{1}{2Q}$	± 470	0.950	18.5°	$87.1/18.5^\circ$	82.6
$\frac{1}{4Q} = \frac{1}{2} \times \frac{1}{2Q}$	± 705	0.900	26.5°	$82.5/26.5^\circ$	73.9
$\frac{1}{2Q} = 1 \times \frac{1}{2Q}$	± 1410	0.707	45.0°	$64.8/45.0^\circ$	45.8
$\frac{1}{Q} = 2 \times \frac{1}{2Q}$	± 2820	0.447	63.5°	$41.0/63.5^\circ$	18.3
$\frac{2}{Q} = 4 \times \frac{1}{2Q}$	± 5640	0.242	76.0°	$22.2/76.0^\circ$	5.4
$\frac{4}{Q} = 8 \times \frac{1}{2Q}$	± 11280	0.124	83.0°	$11.4/83.0^\circ$	1.4
$\frac{8}{Q} = 16 \times \frac{1}{2Q}$	± 22560	0.062	86.5°	$5.7/86.5^\circ$	0.4
$\frac{16}{Q} = 32 \times \frac{1}{2Q}$	± 45120	0.031	88.2°	$2.8/88.2^\circ$	0.1



MU-10227

Figs.25 and 26. Lumped constant parallel circuit.
Locus of the impedance vector.

$$Q_0 = \frac{\omega_0 W_s}{W_d} = \frac{\omega_0 \frac{1}{2} C V^2}{\frac{V^2}{2R}} = \omega_0 C R = \frac{R}{\omega_0 L}$$

Therefore

$$Z = \frac{R + j \frac{R^2}{\omega L} (1 - \omega^2 LC)}{1 + \frac{R^2}{\omega^2 L^2} (1 - \omega^2 LC)^2}$$

$$= \frac{R + jR \left(\frac{\omega_0}{\omega}\right) Q_0 \left[\frac{\omega_0^2 - \omega^2}{\omega_0^2}\right]}{1 + \left(\frac{\omega_0}{\omega}\right)^2 Q_0^2 \left[\frac{\omega_0^2 - \omega^2}{\omega_0}\right]^2}$$

$$Z = R \left[\frac{1 + j Q_0 \left(\frac{\omega_0^2 - \omega^2}{\omega_0 \omega}\right)}{1 + Q_0^2 \left(\frac{\omega_0^2 - \omega^2}{\omega_0 \omega}\right)^2} \right]$$

$$= R \frac{\sqrt{1 - Q_0^2 \left(\frac{\omega_0^2 - \omega^2}{\omega_0 \omega}\right)^2}}{1 + Q_0^2 \left(\frac{\omega_0^2 - \omega^2}{\omega_0 \omega}\right)^2} \quad \theta = \tan^{-1} Q_0 \left(\frac{\omega_0^2 - \omega^2}{\omega_0 \omega}\right)$$

$$= \frac{R}{2} - \frac{R}{2} + R \left[\frac{1 + j Q_0 \left(\frac{\omega_0^2 - \omega^2}{\omega \omega_0}\right)}{1 + Q_0^2 \left(\frac{\omega_0^2 - \omega^2}{\omega \omega_0}\right)^2} \right]$$

$$= \frac{R}{2} + \frac{R}{2} \left[\frac{-1 - Q_0^2 \left(\frac{\omega_0^2 - \omega^2}{\omega_0 \omega}\right) + 2 + j 2 Q_0 \left(\frac{\omega_0^2 - \omega^2}{\omega_0 \omega}\right)}{1 + Q_0^2 \left(\frac{\omega_0^2 - \omega^2}{\omega \omega_0}\right)^2} \right]$$

$$\begin{aligned}
 &= \frac{R}{2} + \frac{R}{2} \left[\frac{\left\{ 1 + jQ_0 \left(\frac{\omega_0^2 - \omega^2}{\omega_0 \omega} \right) \right\} \left\{ 1 + jQ_0 \left(\frac{\omega_0^2 - \omega^2}{\omega_0 \omega} \right) \right\}}{\left\{ 1 + jQ_0 \left(\frac{\omega_0^2 - \omega^2}{\omega_0 \omega} \right) \right\} \left\{ 1 - jQ_0 \left(\frac{\omega_0^2 - \omega^2}{\omega_0 \omega} \right) \right\}} \right] \\
 &= \frac{R}{2} + \frac{R}{2} \left[\frac{1/\theta = \tan^{-1} Q_0 \left(\frac{\omega_0^2 - \omega^2}{\omega_0 \omega} \right) - \tan^{-1} (-) Q_0 \left(\frac{\omega_0^2 - \omega^2}{\omega_0 \omega} \right)}{\phantom{1/\theta = \tan^{-1} Q_0 \left(\frac{\omega_0^2 - \omega^2}{\omega_0 \omega} \right) - \tan^{-1} (-) Q_0 \left(\frac{\omega_0^2 - \omega^2}{\omega_0 \omega} \right)}} \right]
 \end{aligned}$$

But the simple relation between the inverse tangents $\tan^{-1}(-\theta) = +\tan^{-1}\theta$ gives the final result:

$$Z = \frac{R}{2} + \frac{R}{2} \left[\frac{1}{\theta} = 2 \tan^{-1} Q_0 \left(\frac{\omega_0^2 - \omega^2}{\omega_0 \omega} \right) \right],$$

which clearly shows the locus to be a circle.

F. Experimental Data

Results are given in the following tables.

Table X

Q - measurement of pre-exciter No. B grid circuit							
f		$f_0 + \Delta f$		$f_0 - \Delta f$		$2\Delta f$	$Q = \frac{f_0}{2\Delta f}$
Freq. meter	f	Freq. meter	f	Freq. meter	f	(Mc)	
1098.7	207.090	1102.7	207.271	1094.0	206.878	0.393	530
1098.2	207.066	1102.4	207.258	1094.8	206.918	0.340	609
1099.2	207.114	1102.6	207.267	1094.5	206.900	0.367	565
Freq. meter - TS-175/U Ser. 833						$Q_{av} = 568$ 4-4-55 - G. J. E.	

Table XI

Measurement of oscillation characteristics - Cases I, II

Osc dial	Normal operation				$P_o = 0$ (Loop No. 1 nulled)	
	Manual slide- back volt- meter	P_o	Freq. meter	f (Mc)	Freq. meter	f (Mc)
8	33	137	929.2	202.536	936.2	202.856
CW* 6 1/2	0	0	935.8	202.842	----	
CW 2	0	0	936.6	202.873	936.8	202.883
CW 20	0	0	937.4	202.908	937.5	202.914
CW 14	0	0	937.9	202.932	973.9	202.933
CW 8	0	0	938.3	202.950	938.3	202.950
CCW†14	30	113	929.2	202.536	935.5	202.823
CCW 20	27.5	95	929.2	202.536	934.6	202.782
CCW 2	25	79	929.2	202.536	933.6	202.736
CCW 5	0	0	929.2	202.536	----	
CCW 8	0	0	926.3	202.408	927.4	202.456
CCW 14	0	0	925.9	202.392	926.0	202.396
CCW 20	0	0	925.1	202.357	924.9	202.344
CCW 2	0	0	923.7	202.290	923.8	202.300
CCW 8	0	0	922.3	202.229	922.3	202.228

Freq. meter - TS 175/U - Ser. No. 78. 8-13-55 - J. V. F.

* Clockwise

† Counterclockwise

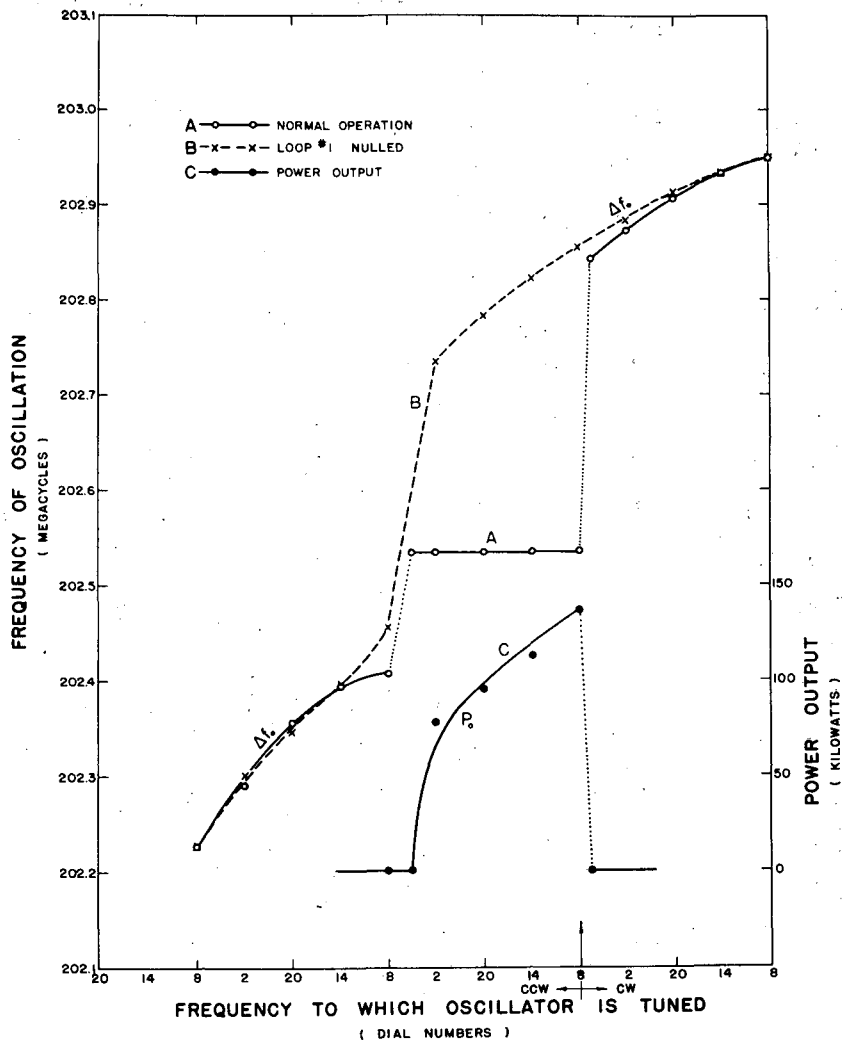
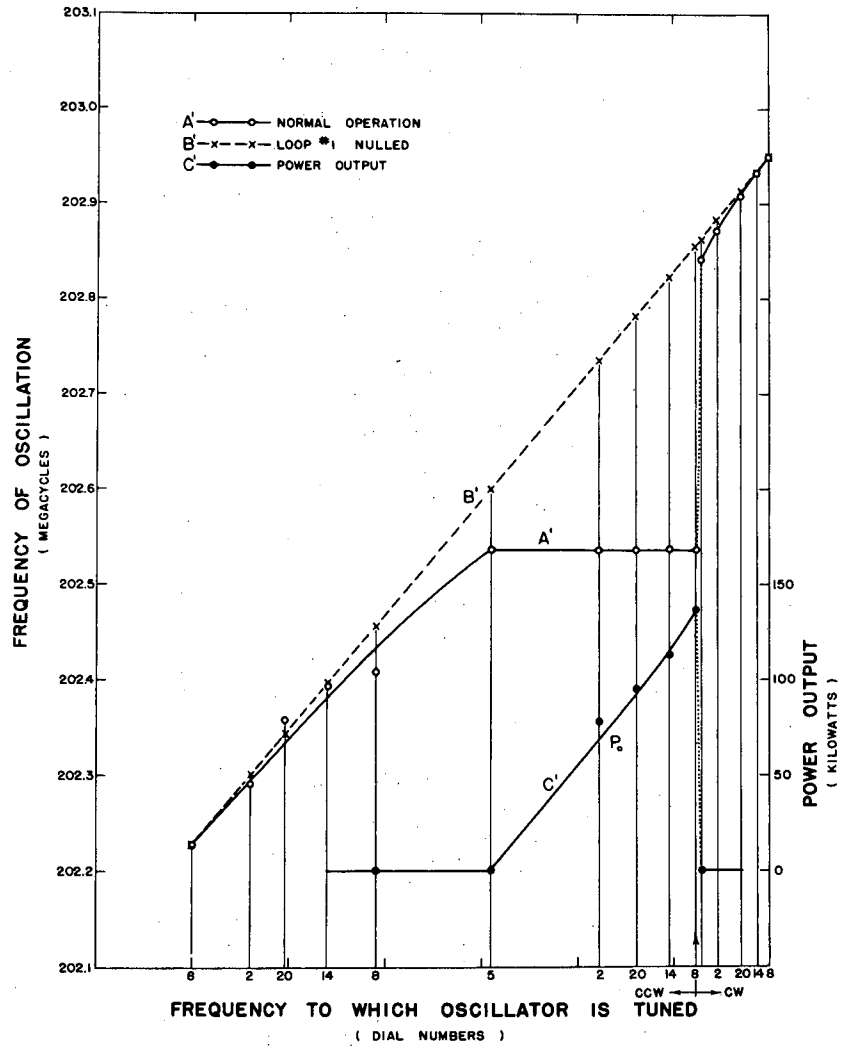


Fig. 27. Frequency of oscillation and power output as functions of the frequency to which the oscillator is tuned: experimental data corresponding to Cases I and II.



MU-10229

Fig. 28. Corrected experimental data corresponding to Cases I and II.

NOTE: The experimental data are plotted against a linear frequency line to correct for the fact that the tuning capacitor varies inversely as the spacing where the spacing is proportional to knob numbers. Also, the calculations do not admit to coupling back through feedback line No. 2 nor do they admit to accidental resonances in the oscillating grid circuit as indicated by the jump in Curve B.

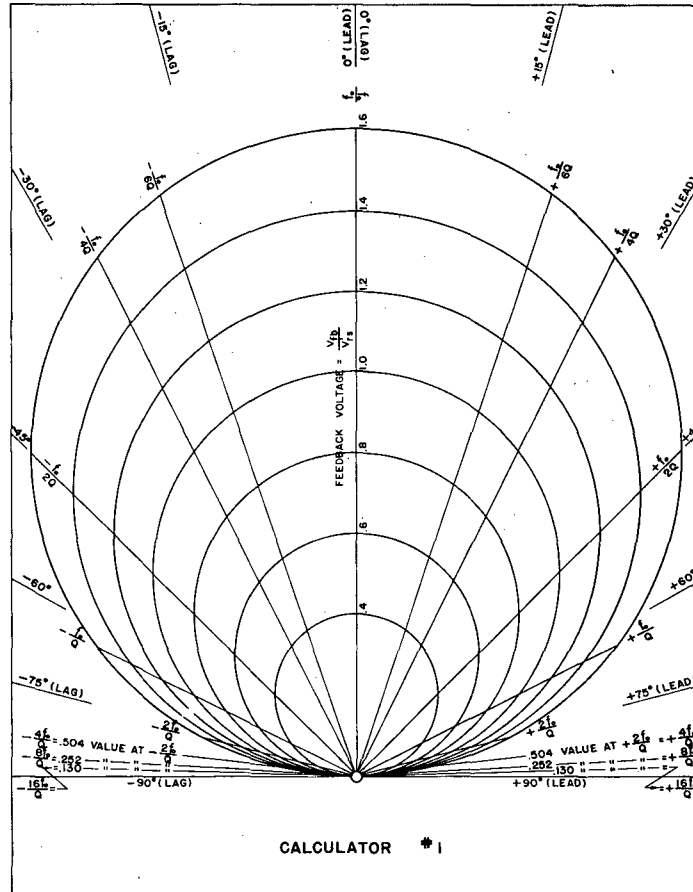
DEFINITIONS OF SYMBOLS

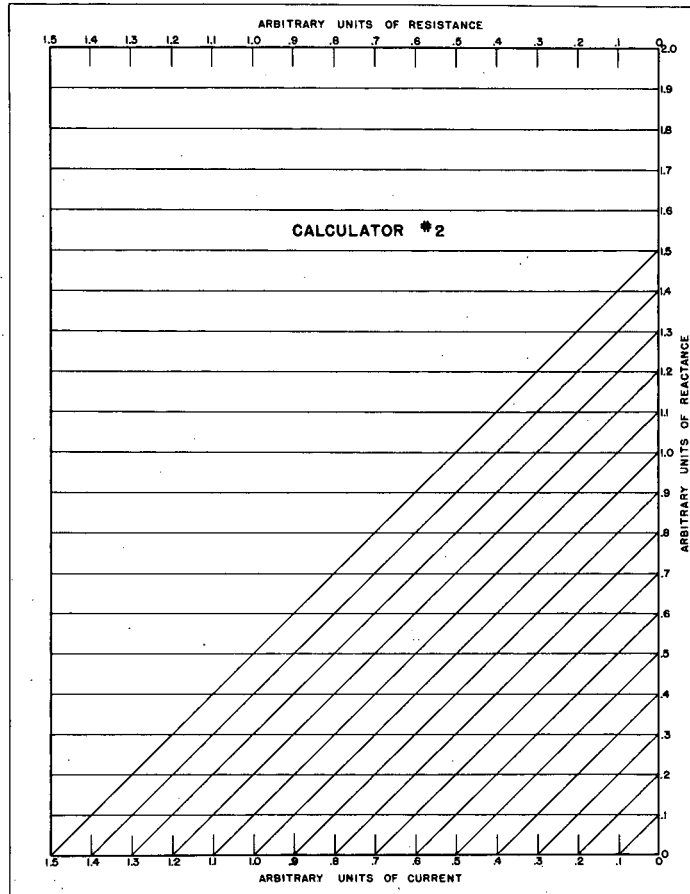
- A_{l1} = area of coupling loop No. 1 (p. 13)
 A_{l2} = area of coupling loop No. 2 (p. 13)
 a = with subscripts, the coefficients of the Fourier series (p. 61)
 b = with subscripts, the coefficients of the Fourier series (p. 61)
 C = capacity (p. 26)
 C' = equivalent lumped circuit capacity of the cathode-grid-screen circuit (p. 17)
 C'' = equivalent shunt capacity appearing across the cathode-grid-screen circuit as a result of the feedback network (p. 23)
 C''' = corrected value of the equivalent shunt capacity appearing across the cathode-grid-screen circuit as a result of the feedback network (p. 26)
 C_o = with additional subscripts, the capacity per meter of transmission line (p. 50)
 c = coupling coefficient (p. 13)
 d_i = diameter of the inner conductor of a coaxial transmission line (p. 53)
 d_o = diameter of the outer conductor of a coaxial transmission line (p. 53)
 E_g = dc . control grid bias (p. 18)
 E_p = dc . plate voltage (p. 56)
 E_s = dc . screen voltage (p. 56)
 e_g = instantaneous value of the grid-to-cathode voltage (p. 58)
 e_{gm} = maximum instantaneous value of the grid-to-cathode voltage (p. 18)
 e_p = instantaneous value of the plate-to-cathode voltage (p. 58)
 e_{pm} = minimum instantaneous value of the plate-to-cathode voltage (p. 56)
 e_s = instantaneous value of the screen-to-cathode voltage (p. 58)
 e_{sm} = minimum instantaneous value of the screen-to-cathode voltage (p. 18)
 $F(t)$ = arbitrary periodic function of time (p. 58 , 61)
 f = frequency in cycles per second
 f_0 = natural frequency of oscillation of the resonant load in cycles per second (p. 21.)
 h = fraction of the plate-to-screen voltage across which transmission line No. 1 is coupled (p. 11)

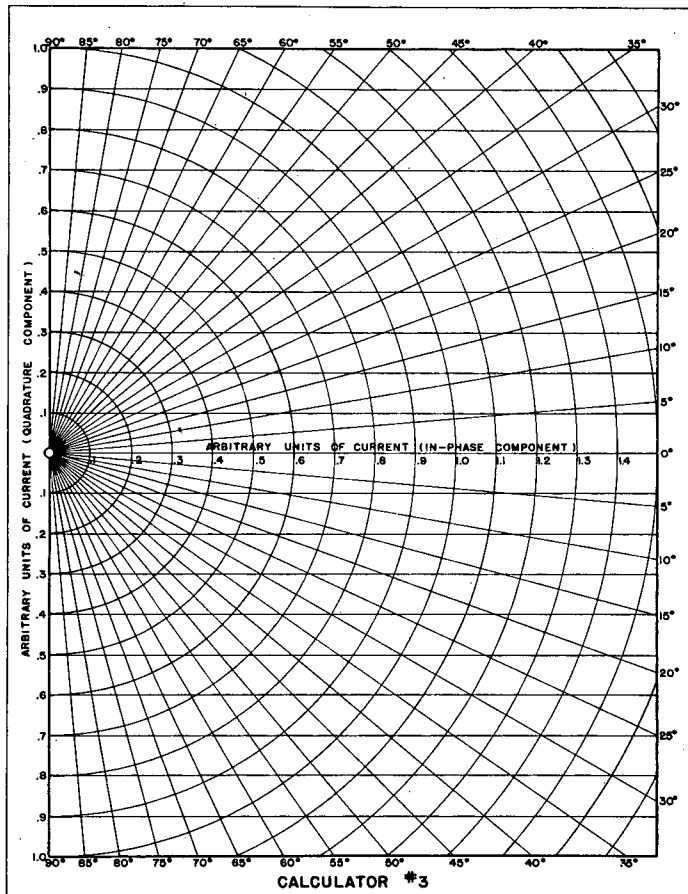
- I = crest value of the fundamental frequency current (p. 52)
- I_g = dc grid current (p. 55)
- I_p = dc plate current (p. 55)
- I_{ps} = crest value of the fundamental frequency component of the plate-screen current (p. 11)
- I_s = dc screen current (p. 57)
- I_{sg} = crest value of the fundamental frequency component of the space current to the plane of the screen (p. 18)
- I'_{sg} = crest value of the fundamental frequency current that is delivered to the cathode-grid-screen circuit by the simple generator used representing the tube (p. 18)
- I_0 = crest value of the fundamental frequency current at the short circuit end of a quarter-wave coaxial resonant circuit (p. 52)
- i_g = instantaneous value of the grid current (p. 59)
- i_p = instantaneous value of the plate current (p. 59)
- i_s = instantaneous value of the screen current (p. 59)
- i_{sg} = instantaneous value of the space current to the plane of the screen (p. 59)
- i_1 = crest value of the network current flowing through the simple generator used to represent the cathode-grid-screen portion of the tube (p. 24)
- i_2 = crest value of the network current flowing through the equivalent grid circuit (p. 24)
- i_3 = crest value of the network current flowing through the simple generator used to represent the feedback circuit (p. 24)
- L = inductance (p. 26)
- ℓ = length in meters (p. 50)
- λ = wavelength in meters (p. 17)
- N = normalizing constant (p. 32)
- n = number of half-wave lengths in transmission line No. 2 (p. 12)
- P_g = grid drive power (p. 64)
- P_o = power output (p. 5)
- Q = 2π times the energy stored divided by the energy dissipated per cycle (p. 4)
- Q_c = calculated value of Q (p. 55)
- Q_m = measured value of Q (p. 55)

- Q_t = composite system Q (p. 17)
- R_g = resistive impedance of the tube grid to cathode (p. 55)
- R_i = resistance per meter of the inner conductor of a coaxial transmission line (p. 52)
- R_o = resistance per meter of the outer conductor of a coaxial transmission line (p. 52)
- R_{ps} = resistive component of the plate-load impedance (p. 5)
- R'_s = shunt resistance of the cathode-grid-screen circuit including grid drive power (p. 17)
- r_s = surface resistivity (ohms per square) (p. 53)
- r_{sc} = screen load impedance (p. 18)
- r'_{sg} = internal impedance of the simple generator used to represent the tube in the cathode-grid-screen circuit of the oscillator (p. 17)
- r_{si} = surface resistivity of the inner conductor of a coaxial transmission line (p. 52)
- r_{so} = surface resistivity of the outer conductor of a coaxial transmission line (p. 52)
- t = time (p. 61)
- V = voltage (p. 50)
- V_{fb} = crest value of the fundamental frequency voltage of the simple generator used to represent the feedback to the grid circuit of the oscillator (p. 11)
- V_g = crest value of the fundamental frequency voltage grid to cathode (p. 18)
- V_{l1} = crest value of the fundamental frequency voltage on loop No. 1 (p. 11)
- V_{l2} = crest value of the fundamental frequency voltage on loop No. 2 (p. 13)
- V_{pc} = crest value of the fundamental frequency voltage plate to cathode (p. 56)
- V_{ps} = crest value of the fundamental frequency voltage plate to screen (p. 5)
- V'_{rs} = crest value of the fundamental frequency voltage across the cathode-grid-screen circuit due to the simple generator used in this circuit to represent the tube (p. 23)
- V_{sc} = crest value of the fundamental frequency voltage screen to cathode (p. 18)
- V_{sg} = crest value of the fundamental frequency voltage screen to grid (p. 18)

- V'_{sg} = crest value of the fundamental frequency voltage of the simple generator used to represent the cathode-grid-screen circuit of the oscillator (p. 15)
- V_0 = with additional subscripts, the crest value of the fundamental frequency voltage at the open end of a coaxial resonant circuit (p. 17)
- W_d = with additional subscripts, power dissipated (p. 17)
- W_{dc} = power dissipated, calculated value (p. 55)
- W_{dm} = power dissipated, measured value (p. 55)
- W_g = power dissipated as a result of the power required to drive the grid of the tube (p. 55)
- W_s = with additional subscripts, energy stored (p. 50)
- Z_{fb} = internal impedance of the simple generator used to represent the voltage fed back to the grid circuit of the oscillator via transmission line No. 2 (p. 13)
- Z_{l1} = coupled impedance of loop No. 1 (p. 13)
- Z_{l2} = coupled impedance of loop No. 2 (p. 14)
- Z_{ps} = load impedance plate to screen (p. 14)
- Z_c = impedance of the coupling between the feedback circuit and the cathode-grid-screen circuit (p. 15)
- Z_{01} = characteristic impedance of the first quarter wavelength of the output transmission line (p. 12)
- Z_{011} = characteristic impedance of the second quarter wavelength of the output transmission line (p. 12)
- Z = with number subscripts, the impedances in the coupling network (p. 14)
- ϵ_1 = dielectric constant of the insulating medium (p. 54)
- θ = angular displacement of the Fourier analysis points from the crest value of the plate, screen and grid voltages (p. 58)
- ω = angular frequency in radius per second (p. 17)
- ω_0 = angular frequency of resonance (p. 65)







BIBLIOGRAPHY

1. R. Adler, "A Study of Locking Phenomena in Oscillators", Proc. Inst. Radio Engrs., 34, 351 - 357, (1946).
2. P.R. Aigram and E.M. Williams, "Pseudosynchronization in Amplitude-Stabilized Oscillators", Proc. Inst. Radio Engrs., 36, 800-801 (1948).
3. L.W. Alvarez, et al., "Berkeley Proton Linear Accelerator," Rev. Sci, Instr. 26, No. 2, 111-133 (1955).
4. E.V. Appleton, "The Automatic Synchronization of Triode Oscillators" Proc. Cambridge Phil. Soc. 21, 231-248 (1922-23).
5. R.D. Huntoon and A. Weiss "Synchronization of Oscillators - Proc. Inst. Radio Engrs., 35, 1415-1423 (1947).
6. S. Ramo and J.R. Whinnery, Fields and Waves in Modern Radio, John Wiley and Sons, 1945.
7. F.E. Terman, Radio Engineers Handbook, McGraw Hill Co., 1943.
8. H.P. Thomas, "Determination of Grid Driving Power in Radio Frequency Power Amplifiers", Proc. Inst. Radio Engrs., 21, 1134-1141 (1933).
9. W.G. Wagner, "Simplified Methods for Computing Performance of Transmitting Tubes", Proc. Inst. Radio Engrs., V.25, ps. 47-77 (1937).

